Self-Constructing Adaptive Robust Fuzzy Neural Tracking Control of Surface Vehicles With Uncertainties and Unknown Disturbances

Ning Wang, *Member, IEEE*, and Meng Joo Er, *Senior Member, IEEE*

***Abstract*— In this paper, a novel self-constructing adaptive robust fuzzy neural control (SARFNC) scheme for tracking surface vehicles, whereby a self-constructing fuzzy neural network (SCFNN) is employed to approximate system uncertainties and unknown disturbances, is proposed. The salient features of the SARFNC scheme are as follows: 1) unlike the predefined-structure approaches, the SCFNN is able to online self-construct dynamic-structure fuzzy neural approximator by generating and pruning fuzzy rules, and achieve accurate approximation; 2) an adaptive approximation-based controller (AAC) is designed by combining sliding-mode control with SCFNN approximation using improved projection-based adaptive laws, which avoid parameter drift and singularity in membership functions simultaneously; 3) to compensate for approximation errors, a robust supervisory controller (RSC) is presented to enhance the robustness of the overall SARFNC control system; and 4) the SARFNC consisting of AAC and RSC can achieve an excellent tracking performance, whereby tracking errors and their first derivatives are globally uniformly ultimately bounded. Simulation studies and comprehensive comparisons with traditional adaptive control schemes demonstrate remarkable performance and superiority of the SARFNC scheme in terms of tracking errors and online approximation.**

***Index Terms*— Adaptive robust tracking control, self-constructing fuzzy neural network (SCFNN), surface vehicle.**

I. Introduction

CONTROL of a surface vehicle has recently attracted a great deal of attention, including, model- and approximation-based approaches [1]. Model-based approaches require system dynamics to be at least partially known so that traditional nonlinear control laws, i.e., feedback linearilization [2], backstepping technique [3], and sliding-mode control (SMC) [4], can be applied. Unfortunately, traditional adaptive control techniques are meaningful only for systems whose nonlinear dynamics and/or uncertainties are linear-in-the-parameter with explicitly defined regressors. Moreover, the surface vehicle dynamics inevitably suffer from complex hydrodynamics, uncertainties, and unknown disturbances with respect to external environments [5], [6], and thereby resulting in great difficulties using traditional control schemes. In this context, the simplified vessel dynamics of [1] has become the nominal model for many model-based design techniques. Holtzhüter [7] developed an adaptive high precision track controller for a linear model through a combination of feedforward and linear quadratic Gaussian feedback control. Considering a nonlinear ship model, Vik and Fossen [8] proposed a semiglobal exponentially stable output feedback control law for automatic heading control where the yaw rate is reconstructed by a linear observer. Wondergem *et al.* [9] extended the foregoing results to an output feedback trajectory tracking control scheme for 3-DOF fully actuated surface ships in the presence of uncertainties. Combining with the traditional input–output linearization strategy, a continuous SMC can be designed to ensure system's robustness and better performance [10]. Recently, the backstepping and sliding-mode techniques have been intensively applied to tracking control of surface vehicles [11]–[13]. In the backstepping framework, Lefeber *et al.* [14] proposed a simple state-feedback control law that renders tracking error dynamics globally exponential stable. Instead of traditional feedback linearization and nonlinearity cancelation, Li *et al.* [15] proposed a feedback dominance-based backstepping controller for a 4-DOF nonlinear model. Using a second-level sliding mode strategy of [16], Yu *et al.* [17] designed a robust tracking controller for an underactuated ship with uncertain parameters.

However, traditional nonlinear controllers are essentially model-based approaches, whereby most of the works mainly focus on mathematical solutions to underactuated or nonholonomic system control while practical uncertainties and disturbances are usually omitted [18]. In this context, previous model-based (adaptive) control methods would inevitably rely on partially or fully known model dynamics since the equivalent control is directly derived from the nonlinearity cancellation or dominance while an additional robustness term is designed to attenuate residual errors. In addition to uncertain

Manuscript received December 26, 2013; revised June 20, 2014; accepted September 5, 2014. Manuscript received in final form September 19, 2014. This work was supported in part by the National Natural Science Foundation of China under Grant 51009017 and Grant 51379002, in part by the Applied Basic Research Funds through the Ministry of Transport of China under Grant 2012-329-225-060, in part by the China Post-Doctoral Science Foundation under Grant 2012M520629, in part by the Program for Liaoning Excellent Talents in University under Grant LJQ2013055, and in part by the Fundamental Research Funds for the Central Universities of China under Grant 2009QN025, Grant 2011JC002, Grant 3132013025, and Grant 3132014206. Recommended by Associate Editor D. Vrabie.

N. Wang is with Marine Engineering College, Dalian Maritime University, Dalian 116026, China (e-mail: n.wang.dmu.cn@gmail.com).

M. J. Er is with the School of Electrical and Electronic Engineering, Nanyang Technological University, Singapore 639798 (e-mail: emjer@ntu.edu.sg).

Color versions of one or more of the figures in this paper are available online at http://ieeexplore.ieee.org.

Digital Object Identifier 10.1109/TCST.2014.2359880

dynamics, unknown external disturbances are actually of greater importance for tracking control of surface vehicles.

In comparison with model-based methods, approximation-based approaches via fuzzy logic systems (FLSs) [19]–[22], neural networks (NNs) [23]–[28], and fuzzy NNs (FNNs) [29]–[32] do not require parametric or functional certainty and have been widely applied to active suspension systems [33], robot manipulators [34], inverted pendulums [35], and Micro-Electro-Mechanical System gyroscope [36]. Due to model uncertainties and unknown disturbances imposed on a surface vehicle, the approximation-based control methods are highly desired to realize online adaptation and robustness to unknown dynamics. In the early stage, researchers have directed much efforts to ship steering control via FLS [37], [38] and NN [39], respectively. Although functional uncertainties could be handled, the scheme considered only the single-input, single-output (SISO) steering equation and neglected the couplings with the surge and sway dynamics. Considering unmodeled dynamics, the NN-based model reference adaptive control scheme was proposed in [40] for trajectory tracking of surface vehicles. Yang and Ren [41] developed an adaptive fuzzy robust tracking control algorithm for a ship autopilot system to maintain the ship on a predetermined heading, whereby stability is guaranteed using the input-to-state stability approach and small gain theorem. Tee and Ge [42] addressed the problem of tracking a desired trajectory for fully actuated ocean vessels by the combination of feedforward NN and domination design techniques, which allow time-varying disturbances to be handled. Recently, Dai *et al.* [43] presented a stable adaptive NN tracking controller for the ocean surface ship in uncertain dynamical environments in the framework of backstepping and Lyapunov synthesis.

In spite of various achievements, the learning ability of the aforementioned adaptive approximation-based control schemes with only output weights being updated is actually limited by the predefined regressors since the weight adaptation is merely required to guarantee stability of the closed-loop system rather than uncertainty identification. In this context, the FNN can enhance the learning capability of FLS by incorporating the NN topology, which allows all free parameters to be adaptively updated according to performance criteria [44], [45]. Note that adaptive laws only consider parameter learning without structure update, i.e., the number of fuzzy rules or hidden nodes must be determined *a priori*, although the resulting performance is acceptable because convergence of the tracking error does not necessarily imply convergence (or even robustness) of the estimated parameters [46]. It implies that the approximation accuracy would be much poorer if inadequate fuzzy rules, i.e., too many or too few, are predefined.

To circumvent the aforementioned problem, Park *et al.* [47], [48] proposed self-structuring NN and FLS control schemes for SISO nonlinear systems, whereby new hidden neurons and fuzzy sets are increasingly created to cover observations, and thereby decreasing approximation errors. However, the resulting architecture and memory storage could grow without bound. Recently, the self-organizing FNN (SOFNN) with structure and parameter updated simultaneously have been proposed in [49]–[51] and references therein, which can automatically generate fuzzy rules in addition to parameter update. It has also attracted researchers to incorporate the SOFNN into adaptive approximation-based control schemes [52]–[55]. Note that the previous SOFNN-based adaptive and robust control methods inevitably suffer from the deficiency that parameter adaptation is rarely able to avoid parameter drift and the singularity problem in that the centers and widths of the membership functions might be updated beyond the universe of discourse and crossing zeros, respectively, if only the norms are assumed to be bounded. In addition, to the best of our knowledge, there does not exist any SOFNN-based control scheme for tracking a surface vehicle.

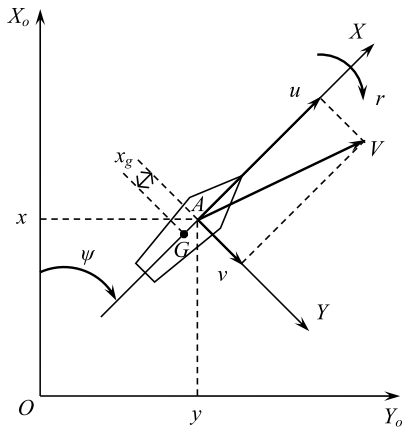

Fig. 1. Earth-fixed OX_oY_o and the body-fixed AXY coordinate frames.

In this paper, a novel self-constructing adaptive robust fuzzy neural control (SARFNC) scheme for tracking surface vehicles in the presence of uncertainties and unknown disturbances is proposed. In the SARFNC scheme, a self-constructing FNN (SCFNN) is developed by dynamically generating and pruning Takagi-Sugeno fuzzy rules according to structure learning criteria. The SCFNN is then used to approximate uncertain dynamics together with unknown external disturbances, and thereby contributing to an SCFNN-based adaptive controller by defining a sliding mode and employing projection-based adaptive laws for centers, widths, and output weights in the SCFNN. It should be emphasized that the proposed adaptive laws ensure that the widths of the membership function are strictly positive and bounded. In addition, a robust supervisory controller (RSC) is designed to suppress the SCFNN-based approximation error. Moreover, the tracking error and its first derivative are proved to be globally uniformly ultimately bounded (GUUB).

The rest of this paper is organized as follows. Section II formulates the trajectory tracking control problem associated with surface vehicles. The SCFNN is addressed in Section III and the SARFNC scheme is presented in Section IV. Simulation studies and comprehensive comparisons are conducted in Section V. The conclusion is drawn in Section VI.

II. Problem Formulation

As shown in Fig. 1, the earth-fixed frame OX_oY_o and the body-fixed frame AXY of surface vehicles are commonly

used to clearly formulate the problem to be resolved in this paper. The axes OX_o and OY_o are directed to the north and east, respectively, while axes AX and AY are directed to fore and starboard, respectively. Assuming that the vessel is port-starboard symmetric, the distance x_g between the geometric center A and the gravity center G is allocated along the axis AX. Let $\boldsymbol{\eta} = [x, y, \psi]^T$ be the 3-DOF position (x, y) and heading angle (ψ) of the vessel in the earth-fixed inertial frame, and let $\boldsymbol{\nu} = [u, v, r]^T$ be the corresponding linear velocities (u, v), i.e., surge and sway velocities, and angular rate (r), i.e., yaw, in the body-fixed frame. The dynamic model of the surface vehicle can be described as follows:

$$\dot{\boldsymbol{\eta}} = \mathbf{R}(\psi)\boldsymbol{\nu} \tag{1a}$$

$$\mathbf{M}\dot{\boldsymbol{\nu}} + \mathbf{C}(\boldsymbol{\nu})\boldsymbol{\nu} + \mathbf{D}(\boldsymbol{\nu})\boldsymbol{\nu} = \boldsymbol{\tau} + \mathbf{R}^T(\psi)\mathbf{b} \tag{1b}$$

where $\boldsymbol{\tau} = [\tau_1, \tau_2, \tau_3]^T$ and $\mathbf{b}(t) = [b_1(t), b_2(t), b_3(t)]^T$ are the control input and unknown time-varying dynamics and external disturbances due to wind, waves, and ocean currents in the body-fixed frame, respectively, and the matrix $\mathbf{R}(\psi)$ is the 3-DOF rotation matrix given by

$$\mathbf{R}(\psi) = \begin{bmatrix} \cos\psi & -\sin\psi & 0 \\ \sin\psi & \cos\psi & 0 \\ 0 & 0 & 1 \end{bmatrix} \tag{2}$$

with the following properties:

$$\mathbf{R}^T(\psi)\mathbf{R}(\psi) = \mathbf{I}, \quad \|\mathbf{R}(\psi)\| = 1 \quad \forall\ \psi \in [0, 2\pi]. \tag{3}$$

Furthermore, the inertia matrix $\mathbf{M} = \mathbf{M}^T > 0$, the skew-symmetric matrix $\mathbf{C}(\boldsymbol{\nu}) = -\mathbf{C}(\boldsymbol{\nu})^T$ of Coriolis and centripetal terms and the damping matrix $\mathbf{D}(\boldsymbol{\nu})$ are given by

$$\mathbf{M} = \begin{bmatrix} m_{11} & 0 & 0 \\ 0 & m_{22} & m_{23} \\ 0 & m_{32} & m_{33} \end{bmatrix} \tag{4a}$$

$$\mathbf{C}(\boldsymbol{\nu}) = \begin{bmatrix} 0 & 0 & c_{13}(\boldsymbol{\nu}) \\ 0 & 0 & c_{23}(\boldsymbol{\nu}) \\ -c_{13}(\boldsymbol{\nu}) & -c_{23}(\boldsymbol{\nu}) & 0 \end{bmatrix} \tag{4b}$$

$$\mathbf{D}(\boldsymbol{\nu}) = \begin{bmatrix} d_{11}(\boldsymbol{\nu}) & 0 & 0 \\ 0 & d_{22}(\boldsymbol{\nu}) & d_{23}(\boldsymbol{\nu}) \\ 0 & d_{32}(\boldsymbol{\nu}) & d_{33}(\boldsymbol{\nu}) \end{bmatrix} \tag{4c}$$

where $m_{11} = m - X_{\dot{u}}$, $m_{22} = m - Y_{\dot{v}}$, $m_{23} = mx_g - Y_{\dot{r}}$, $m_{32} = mx_g - N_{\dot{v}}$, $m_{33} = I_z - N_{\dot{r}}$; $c_{13}(\boldsymbol{\nu}) = -m_{11}v - m_{23}r$, $c_{23}(\boldsymbol{\nu}) = m_{11}u$; $d_{11}(\boldsymbol{\nu}) = -X_u - X_{|u|u}|u| - X_{uuu}u^2$, $d_{22}(\boldsymbol{\nu}) = -Y_v - Y_{|v|v}|v| - Y_{|r|v}|r|$, $d_{23}(\boldsymbol{\nu}) = -Y_r - Y_{|v|r}|v| - Y_{|r|r}|r|$, $d_{32}(\boldsymbol{\nu}) = -N_v - N_{|v|v}|v| - N_{|r|v}|r|$, and $d_{33}(\boldsymbol{\nu}) = -N_r - N_{|v|r}|v| - N_{|r|r}|r|$. Here, m is the mass of the vessel, I_z is the moment of inertia about the yaw rotation, and terms X_*, Y_*, and N_* denote the corresponding hydrodynamic derivatives.

By substituting (1a) into (1b), the dynamic model (1a)–(1b) can be rewritten in the following affine nonlinear form:

$$\ddot{\boldsymbol{\eta}} = \mathbf{f}(\boldsymbol{\eta}, \dot{\boldsymbol{\eta}}) + \mathbf{G}(\boldsymbol{\eta})\boldsymbol{\tau} \tag{5}$$

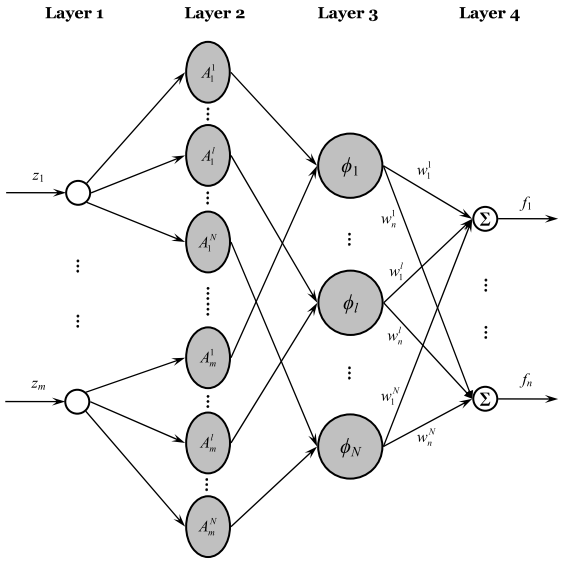

Fig. 2. Architecture of the SCFNN.

where

$$\mathbf{f}(\boldsymbol{\eta}, \dot{\boldsymbol{\eta}}) = \mathbf{f}_0(\boldsymbol{\eta}, \dot{\boldsymbol{\eta}}) + \Delta\mathbf{f}(\boldsymbol{\eta}, t) \tag{6a}$$

$$\mathbf{G}(\boldsymbol{\eta}) = \mathbf{R}(\psi)\mathbf{M}^{-1} \tag{6b}$$

$$\mathbf{f}_0(\boldsymbol{\eta}, \dot{\boldsymbol{\eta}}) = -\mathbf{R}(\psi)\begin{pmatrix} \mathbf{S}^T(\dot{\psi}) + \mathbf{M}^{-1} \\ \times[\mathbf{C}(\mathbf{R}^T(\psi)\dot{\boldsymbol{\eta}}) \\ +\mathbf{D}(\mathbf{R}^T(\psi)\dot{\boldsymbol{\eta}})] \end{pmatrix}\mathbf{R}^T(\psi)\dot{\boldsymbol{\eta}} \tag{6c}$$

$$\Delta\mathbf{f}(\boldsymbol{\eta}, t) = \mathbf{R}(\psi)\mathbf{M}^{-1}\mathbf{R}^T(\psi)\mathbf{b}(t) \tag{6d}$$

$$\mathbf{S}(\dot{\psi}) = \begin{bmatrix} 0 & -\dot{\psi} & 0 \\ \dot{\psi} & 0 & 0 \\ 0 & 0 & 0 \end{bmatrix}. \tag{6e}$$

Remark 1: The smooth vector field $\mathbf{f}$ is implicitly unknown and is perturbed by time-varying external disturbances, while the input matrix $\mathbf{G} > 0$ is known since the rotation matrix $\mathbf{R}$ is explicitly defined by (2) and the inertia matrix $\mathbf{M}$ is usually assumed to be available. In other words, all parametric uncertainties and unknown dynamics have been encapsulated into the nonlinearity $\mathbf{f}(\cdot)$.

In this context, the objective of this paper is to design a self-constructing fuzzy neural control scheme for tracking the surface vehicle (5) with the ability to online identify the lumped unknown dynamics $\mathbf{f}(\cdot)$, such that $\boldsymbol{\eta}$ and $\dot{\boldsymbol{\eta}}$ of the surface vehicle can track arbitrary smooth reference trajectory $\boldsymbol{\eta}_d$ and its first derivative $\dot{\boldsymbol{\eta}}_d$, respectively.

III. Self-Constructing FNN

In this section, we present the SCFNN with dynamically evolving structure to accurately capture unknown nonlinear dynamics including uncertainties and disturbances, i.e., $\mathbf{f}(\mathbf{z})$ in (5), where $\mathbf{z} = [\boldsymbol{\eta}^T, \dot{\boldsymbol{\eta}}^T]^T = [z_1, z_2, \ldots, z_m]^T$.

A. Architecture

As shown in Fig. 2, the SCFNN is comprised of four layers, i.e., input, membership, rule, and output layers, which

contribute to the fuzzy rule base as follows:

$$\text{IF } z_i \text{ is } A_i^l, \text{ THEN } f_j(\mathbf{z}) = w_j^l, \quad l = 1, 2, \ldots, N \tag{7}$$

where $A_i^l, i = 1, 2, \ldots, m$ and $w_j^l, j = 1, 2, \ldots, n$ are input fuzzy sets and output fuzzy singletons, respectively. The overall output of the SCFNN can be obtained as follows:

$$\mathbf{f}_F(\mathbf{z}) = [f_1, f_2, \ldots, f_n]^T = \mathbf{W}^T \boldsymbol{\Phi}(\mathbf{z}; \mathbf{c}, \boldsymbol{\sigma}) \tag{8}$$

where $\mathbf{f}_F : U_\mathbf{z} \subset \mathbf{R}^m \to \mathbf{R}^n$, and the output weight matrix $\mathbf{W}$ and regressor vector $\boldsymbol{\Phi}(\mathbf{z}; \mathbf{c}, \boldsymbol{\sigma})$ are defined as follows:

$$\mathbf{W} = [\boldsymbol{\omega}_1, \ldots, \boldsymbol{\omega}_n] \in \mathbf{R}^{N \times n}, \ \boldsymbol{\omega}_j = \left[w_j^1, \ldots, w_j^N\right]^T \tag{9}$$

$$\boldsymbol{\Phi} = [\phi_1, \phi_2, \ldots, \phi_N]^T \in \mathbf{R}^N. \tag{10}$$

Here, the fuzzy basis function (FBF) is defined by

$$\phi_l = \exp\left(-(\mathbf{z} - \mathbf{c}_l)^T \boldsymbol{\Sigma}_l^{-2} (\mathbf{z} - \mathbf{c}_l)\right) \tag{11}$$

where $\boldsymbol{\Sigma}_l = \text{diag}(\sigma_1^l, \ldots, \sigma_m^l) \in \mathbf{R}^{m \times m}$, $\mathbf{c} = [\mathbf{c}_1^T, \ldots, \mathbf{c}_N^T]^T \in \mathbf{R}^{mN}$, and $\mathbf{c}_l = [c_1^l, \ldots, c_m^l]^T$ are FBF center vectors and $\boldsymbol{\sigma} = [\boldsymbol{\sigma}_1^T, \ldots, \boldsymbol{\sigma}_N^T]^T \in \mathbf{R}^{mN}$ and $\boldsymbol{\sigma}_l = [\sigma_1^l, \ldots, \sigma_m^l]^T$ are the FBF width vectors. All parameters are bounded on $U_\mathbf{z}$ and the width of a fuzzy set is positive

$$\|\boldsymbol{\omega}_j\| \le \overline{\omega}_j, \quad \underline{c}_i \le c_i^l \le \overline{c}_i, \quad 0 < \underline{\sigma}_i \le \sigma_i^l \le \overline{\sigma}_i. \tag{12}$$

Without loss of generality, assume that there exists an optimal fuzzy approximator with N^* fuzzy rules that can identify the nonlinear function $\mathbf{f}(\mathbf{z})$ with the minimal functional approximation error (MFAE)

$$\mathbf{f}(\mathbf{z}) = (\mathbf{W}^*)^T \boldsymbol{\Phi}(\mathbf{z}; \mathbf{c}^*, \boldsymbol{\sigma}^*) + \boldsymbol{\varepsilon}_f^*(\mathbf{z}) \tag{13}$$

where the MFAE $\boldsymbol{\varepsilon}_f^*(\mathbf{z}) = [\varepsilon_{f,1}^*, \varepsilon_{f,2}^*, \ldots, \varepsilon_{f,n}^*]^T \in \mathbf{R}^n$ is usually bounded on $U_\mathbf{z}$, i.e., $|\varepsilon_{f,j}^*| \le \overline{\varepsilon}_{f,j}$, and

$$(\mathbf{W}^*, \mathbf{c}^*, \boldsymbol{\sigma}^*) = \arg \min_{(\mathbf{W}, \mathbf{c}, \boldsymbol{\sigma})} \left(\max_{\mathbf{z} \in U_\mathbf{z}} \|\mathbf{f}_\mathrm{F}(\mathbf{z}; \mathbf{W}, \mathbf{c}, \boldsymbol{\sigma}) - \mathbf{f}(\mathbf{z})\| \right). \tag{14}$$

Remark 2: The structure of traditional fuzzy or neural approximators used in the control paradigm is usually predefined by trials and errors while only parameters are updated by adaptive laws, and thereby leading to fixed-structure identifier [46] and arising inaccurate identification due to mismatched fuzzy rules or feature mappings. For surface vehicles with high frequency and large scale disturbances, the dynamic-structure fuzzy neural identifier for complex dynamics is highly desired.

B. Self-Constructing Scheme

Let $\mathbf{c}^i = [c_i^1, c_i^2, \ldots, c_i^N]^T$ and $\boldsymbol{\sigma}^i = [\sigma_i^1, \sigma_i^2, \ldots, \sigma_i^N]^T$ be the center and width vectors of the generated fuzzy sets in the ith dimension $z_i(t)$ individually, where $\underline{c}_i \le c_i^l \le \overline{c}_i$, $0 < \underline{\sigma}_i \le \sigma_i^l \le \overline{\sigma}_i, i = 1, 2, \ldots, m, l = 1, 2, \ldots, N$. The SCFNN begins with no fuzzy rule, i.e., $\mathbf{c}^i(0) = \emptyset$, $\boldsymbol{\sigma}^i(0) = \emptyset$, $\boldsymbol{\omega}_j(0) = \emptyset$, and $N(0) = 0$, and generates new fuzzy rules or prunes redundant ones according to the novelty of current observation $\mathbf{z}(t)$ to existing FBFs, i.e., $\mathbf{c}^i(t-1) = [c_i^1, c_i^2, \ldots, c_i^{N(t-1)}]^T$ and $\boldsymbol{\sigma}^i(t-1) = [\sigma_i^1, \sigma_i^2, \ldots, \sigma_i^{N(t-1)}]^T$.

Calculate the generalized distance between $\mathbf{z}(t)$ and the existing FBFs as follows:

$$d^l = (\mathbf{z}(t) - \mathbf{c}_l(t-1))^T \boldsymbol{\Sigma}_l^{-2}(t-1)(\mathbf{z}(t) - \mathbf{c}_l(t-1)), \quad l = 1, 2, \ldots, N(t-1) \tag{15}$$

where $\mathbf{c}_l(t-1) = [c_1^{l(t-1)}, c_2^{l(t-1)}, \ldots, c_m^{l(t-1)}]^T$ and $\boldsymbol{\Sigma}_l(t-1) = \text{diag}(\sigma_1^{l(t-1)}, \sigma_2^{l(t-1)}, \ldots, \sigma_m^{l(t-1)})$.

1) Generation of Rule: Find the nearest fuzzy rule as follows:

$$d_{\min} = \min_{l=1,2,\ldots,N(t-1)} d^l. \tag{16}$$

If

$$d_{\min} > d_{\min}^{\text{th}} \tag{17}$$

there does not exist any fuzzy rule representing the current input. A new FBF needs to be generated

$$\mathbf{c}_{N(t)} = \mathbf{z}(t), \ \boldsymbol{\sigma}_{N(t)} = \boldsymbol{\sigma}_{\text{init}}, \ \mathbf{w}_{N(t)} = \mathbf{0}$$
$$N(t) = N(t-1) + 1. \tag{18}$$

Here, $d_{\min}^{\text{th}}$ is the user-defined threshold and can be easily chosen as $d_{\min}^{\text{th}} = \ln(1/\epsilon), 0 < \epsilon \le 1$, such that the dominant firing strength is no less than ϵ, and $\boldsymbol{\sigma}_{\text{init}}$ is the initial width for the newly generated FBF. Otherwise, no new fuzzy rule will be generated, i.e., $N(t) = N(t-1)$.

2) Pruning of Rule: Find the redundant FBFs sequentially as follows:

$$J_r = \{l^\circ\}, \quad d^{l^\circ} < d_0. \tag{19}$$

If

$$J_r \ne \emptyset \tag{20}$$

redundant fuzzy rules will be pruned as follows:

$$\mathbf{c}_{l^\circ} = \emptyset, \quad \boldsymbol{\sigma}_{l^\circ} = \emptyset, \quad \mathbf{w}_{l^\circ} = \emptyset, \quad N(t) = N(t) - |J_r|, \quad l^\circ \in J_r. \tag{21}$$

Here, d_0 is the user-defined threshold under which the fuzzy rule is considered to be inactive, and is simply chosen as $d_0 = \ln(1/\varsigma), 0 < \varsigma \le 1$.

IV. Self-Constructing Adaptive Robust Fuzzy Neural Control

As shown in Fig. 3, the SARFNC scheme is proposed for tracking the surface vehicle (5) by employing two controllers, i.e., adaptive approximation-based controller (AAC) and RSC.

A. Structure of the SARFNC

Define a sliding surface of the tracking error as follows:

$$\mathbf{s} = \dot{\mathbf{e}} + \mathbf{K}_2 \mathbf{e} + \mathbf{K}_1 \int_0^t \mathbf{e}(\tau) d\tau \tag{22}$$

where $\mathbf{s} = [s_1, \ldots, s_n]^T \in \mathbf{R}^n$, $\mathbf{K}_i = \text{diag}(k_{i1}, \ldots, k_{in}) \in \mathbf{R}^{n \times n}$, and $\mathbf{e} = \boldsymbol{\eta} - \boldsymbol{\eta}_d$ is the tracking error. Accordingly, the SARFNC framework is designed as follows:

$$\boldsymbol{\tau}_{\text{SARFNC}} = \boldsymbol{\tau}_{\text{aac}} + \boldsymbol{\tau}_{\text{rsc}} \tag{23}$$

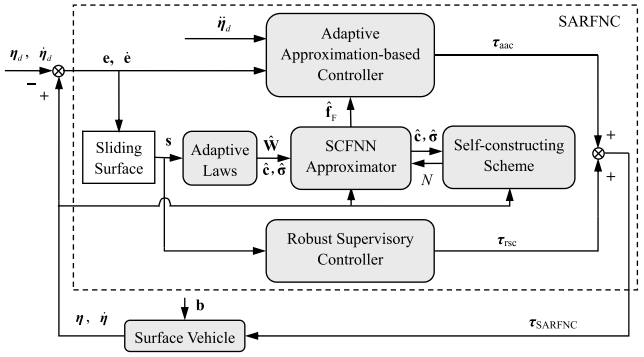

Fig. 3. Block diagram of the SARFNC.

where

$$\boldsymbol{\tau}_{\text{aac}} = \mathbf{M}\mathbf{R}^T(\psi)\big[-\widehat{\mathbf{f}}_{\text{F}}\left(\mathbf{z};\widehat{\mathbf{W}},\widehat{\mathbf{c}},\widehat{\boldsymbol{\sigma}}\right)+\ddot{\boldsymbol{\eta}}_d-\mathbf{K}\underline{\mathbf{e}}\big] \tag{24}$$

$$\boldsymbol{\tau}_{\text{rsc}} = \mathbf{M}\mathbf{R}^T(\psi)\Big[-\frac{\delta^2+1}{2\delta^2}\boldsymbol{\Gamma}\mathbf{s}\Big]. \tag{25}$$

Here, $\mathbf{K}=[\mathbf{K}_1,\mathbf{K}_2]\in\mathbf{R}^{n\times m}$, $\underline{\mathbf{e}}=[\mathbf{e}^T,\dot{\mathbf{e}}^T]^T\in\mathbf{R}^m$, $\boldsymbol{\Gamma}=\text{diag}(\gamma_1,\ldots,\gamma_n)>0$, $\delta\neq 0$ is a constant, and $\widehat{\mathbf{f}}_{\text{F}}(\mathbf{z};\widehat{\mathbf{W}},\widehat{\mathbf{c}},\widehat{\boldsymbol{\sigma}})$ is the SCFNN-based approximator, which is parameterized by $\widehat{\mathbf{W}},\widehat{\mathbf{c}},\widehat{\boldsymbol{\sigma}}$ and derived from the adaptive laws described in Section IV-C.

B. SCFNN-Based Approximation

In the SARFNC scheme (23), the unknown dynamics $\mathbf{f}(\mathbf{z})$ is online identified by the SCFNN with adaptive parameters and dynamic structure (13) using $N(t)$ fuzzy rules as follows:

$$\mathbf{f}(\mathbf{z}) = \widehat{\mathbf{W}}^T\boldsymbol{\Phi}\left(\mathbf{z};\widehat{\mathbf{c}},\widehat{\boldsymbol{\sigma}}\right)+\widehat{\boldsymbol{\varepsilon}}_f(\mathbf{z}) \tag{26}$$

where $\widehat{\mathbf{W}}\in\mathbf{R}^{N\times n}$, $\widehat{\mathbf{c}}\in\mathbf{R}^{mN}$, and $\widehat{\boldsymbol{\sigma}}\in\mathbf{R}^{mN}$ are the estimated parameters, and $\widehat{\boldsymbol{\varepsilon}}_f$ is the approximation error determined by

$$\widehat{\boldsymbol{\varepsilon}}_f = (\mathbf{W}^*)^T\boldsymbol{\Phi}^*-\widehat{\mathbf{W}}^T\widehat{\boldsymbol{\Phi}}+\boldsymbol{\varepsilon}_f^* \tag{27}$$

with $\boldsymbol{\Phi}^*=\boldsymbol{\Phi}\left(\mathbf{z};\mathbf{c}^*,\boldsymbol{\sigma}^*\right)\in\mathbf{R}^{N^*}$ and $\widehat{\boldsymbol{\Phi}}=\boldsymbol{\Phi}\left(\mathbf{z};\widehat{\mathbf{c}},\widehat{\boldsymbol{\sigma}}\right)\in\mathbf{R}^N$. Without loss of generality, assume that $N^*\geq N$ and $(\mathbf{W}^*)^T\boldsymbol{\Phi}^*=(\mathbf{W}_1^*)^T\boldsymbol{\Phi}_1^*+(\mathbf{W}_2^*)^T\boldsymbol{\Phi}_2^*$, where $\mathbf{W}_1^*\in\mathbf{R}^{N\times n},\boldsymbol{\Phi}_1^*=\boldsymbol{\Phi}\left(\mathbf{z};\mathbf{c}_1^*,\boldsymbol{\sigma}_1^*\right)\in\mathbf{R}^N$, $\mathbf{W}_2^*\in\mathbf{R}^{(N^*-N)\times n}$, and $\boldsymbol{\Phi}_2^*=\boldsymbol{\Phi}\left(\mathbf{z};\mathbf{c}_2^*,\boldsymbol{\sigma}_2^*\right)\in\mathbf{R}^{N^*-N}$. From (27), we have

$$\widehat{\boldsymbol{\varepsilon}}_f = \widetilde{\mathbf{W}}^T\left(\widehat{\boldsymbol{\Phi}}+\widetilde{\boldsymbol{\Phi}}\right)+\widehat{\mathbf{W}}^T\widetilde{\boldsymbol{\Phi}}+\widehat{\boldsymbol{\varepsilon}}_f^* \tag{28}$$

where $\widehat{\boldsymbol{\varepsilon}}_f^*=(\mathbf{W}_2^*)^T\boldsymbol{\Phi}_2^*+\boldsymbol{\varepsilon}_f^*$ is the actual functional approximation error, $\widetilde{\mathbf{W}}=\mathbf{W}_1^*-\widehat{\mathbf{W}}$ and $\widetilde{\boldsymbol{\Phi}}=\boldsymbol{\Phi}_1^*-\widehat{\boldsymbol{\Phi}}$ are the output weight and regressor errors, respectively. By applying the Taylor series expansion of $\boldsymbol{\Phi}(\cdot)$ to $(\widehat{\mathbf{c}},\widehat{\boldsymbol{\sigma}})$ in (28), we have

$$\begin{aligned}\widehat{\boldsymbol{\varepsilon}}_f &= \widetilde{\mathbf{W}}^T\widehat{\boldsymbol{\Phi}}+\widehat{\mathbf{W}}^T\left(\boldsymbol{\Phi}_{\mathbf{c}}'\widetilde{\mathbf{c}}+\boldsymbol{\Phi}_{\boldsymbol{\sigma}}'\widetilde{\boldsymbol{\sigma}}+\mathbf{h}(\mathbf{z};\widetilde{\mathbf{c}},\widetilde{\boldsymbol{\sigma}})\right)+\widetilde{\mathbf{W}}^T\widetilde{\boldsymbol{\Phi}}+\widehat{\boldsymbol{\varepsilon}}_f^*\\ &= \widetilde{\mathbf{W}}^T\widehat{\boldsymbol{\Phi}}+\widehat{\mathbf{W}}^T\boldsymbol{\Phi}_{\mathbf{c}}'\widetilde{\mathbf{c}}+\widehat{\mathbf{W}}^T\boldsymbol{\Phi}_{\boldsymbol{\sigma}}'\widetilde{\boldsymbol{\sigma}}+\widehat{\mathbf{W}}^T\mathbf{h}(\mathbf{z};\widetilde{\mathbf{c}},\widetilde{\boldsymbol{\sigma}})\\ &\quad+\widetilde{\mathbf{W}}^T\widetilde{\boldsymbol{\Phi}}+\widehat{\boldsymbol{\varepsilon}}_f^*\\ &= \widetilde{\mathbf{W}}^T\widehat{\boldsymbol{\Phi}}+\widehat{\mathbf{W}}^T\boldsymbol{\Phi}_{\mathbf{c}}'\widetilde{\mathbf{c}}+\widehat{\mathbf{W}}^T\boldsymbol{\Phi}_{\boldsymbol{\sigma}}'\widetilde{\boldsymbol{\sigma}}+\boldsymbol{\varepsilon}_f\end{aligned} \tag{29}$$

where $\widetilde{\mathbf{c}}=\mathbf{c}_1^*-\widehat{\mathbf{c}}$, $\widetilde{\boldsymbol{\sigma}}=\boldsymbol{\sigma}_1^*-\widehat{\boldsymbol{\sigma}}$, and $\mathbf{h}(\mathbf{z};\widetilde{\mathbf{c}},\widetilde{\boldsymbol{\sigma}})$ is the high-order term, and $\boldsymbol{\Phi}_{\mathbf{c}}'$ and $\boldsymbol{\Phi}_{\boldsymbol{\sigma}}'$ are Jacobian matrices given by

$$\boldsymbol{\Phi}_{\mathbf{c}}' \triangleq \frac{\partial\boldsymbol{\Phi}}{\partial\mathbf{c}}\Big|_{\substack{\mathbf{c}=\widehat{\mathbf{c}}\\ \boldsymbol{\sigma}=\widehat{\boldsymbol{\sigma}}}} = \text{diag}\left(\boldsymbol{\phi}_{\mathbf{c}_1}^T,\ldots,\boldsymbol{\phi}_{\mathbf{c}_N}^T\right)\in\mathbf{R}^{N\times mN} \tag{30}$$

$$\boldsymbol{\Phi}_{\boldsymbol{\sigma}}' \triangleq \frac{\partial\boldsymbol{\Phi}}{\partial\boldsymbol{\sigma}}\Big|_{\substack{\mathbf{c}=\widehat{\mathbf{c}}\\ \boldsymbol{\sigma}=\widehat{\boldsymbol{\sigma}}}} = \text{diag}\left(\boldsymbol{\phi}_{\boldsymbol{\sigma}_1}^T,\ldots,\boldsymbol{\phi}_{\boldsymbol{\sigma}_N}^T\right)\in\mathbf{R}^{N\times mN}. \tag{31}$$

Here, $\boldsymbol{\phi}_{\mathbf{c}_l}^T\triangleq\partial\phi_l/\partial\mathbf{c}_l^T=[\partial\phi_l/\partial c_1^l,\ldots,\partial\phi_l/\partial c_m^l]$ and $\boldsymbol{\phi}_{\boldsymbol{\sigma}_l}^T\triangleq\partial\phi_l/\partial\boldsymbol{\sigma}_l^T=[\partial\phi_l/\partial\sigma_1^l,\ldots,\partial\phi_l/\partial\sigma_m^l]$. From (11), we obtain

$$\boldsymbol{\phi}_{\mathbf{c}_l}^T \triangleq \left[\phi_1^{c,l},\ldots,\phi_m^{c,l}\right] = 2\widehat{\phi}_l\left[\frac{z_1-\widehat{c}_1^l}{\left(\widehat{\sigma}_1^l\right)^2},\ldots,\frac{z_m-\widehat{c}_m^l}{\left(\widehat{\sigma}_m^l\right)^2}\right] \tag{32}$$

$$\boldsymbol{\phi}_{\boldsymbol{\sigma}_l}^T \triangleq \left[\phi_1^{\sigma,l},\ldots,\phi_m^{\sigma,l}\right] = 2\widehat{\phi}_l\left[\frac{\left(z_1-\widehat{c}_1^l\right)^2}{\left(\widehat{\sigma}_1^l\right)^3},\ldots,\frac{\left(z_m-\widehat{c}_m^l\right)^2}{\left(\widehat{\sigma}_m^l\right)^3}\right] \tag{33}$$

and $\boldsymbol{\varepsilon}_f$ is the residual approximation error given by

$$\boldsymbol{\varepsilon}_f = \widehat{\mathbf{W}}^T\mathbf{h}(\mathbf{z};\widetilde{\mathbf{c}},\widetilde{\boldsymbol{\sigma}})+\widetilde{\mathbf{W}}^T\widetilde{\boldsymbol{\Phi}}+\widehat{\boldsymbol{\varepsilon}}_f^*. \tag{34}$$

Theorem 1: Consider the SCFNN-based approximation $\widehat{\mathbf{W}}^T\boldsymbol{\Phi}(\mathbf{z};\widehat{\mathbf{c}},\widehat{\boldsymbol{\sigma}})$ to the vessel dynamics $\mathbf{f}(\mathbf{z}),\mathbf{z}\in U_{\mathbf{z}}$, the residual approximation error (34) admits the following boundedness:

$$\boldsymbol{\varepsilon}_f^T\boldsymbol{\varepsilon}_f\leq\frac{8d_0\overline{w}^2}{\underline{\sigma}^2}\widetilde{\mathbf{c}}^T\widetilde{\mathbf{c}}+\frac{8d_0^2\overline{w}^2}{\underline{\sigma}^2}\widetilde{\boldsymbol{\sigma}}^T\widetilde{\boldsymbol{\sigma}}+2\text{tr}\left(\widetilde{\mathbf{W}}^T\widetilde{\mathbf{W}}\right)+\Delta d<\infty \tag{35}$$

where $\Delta d=5\overline{w}^2+4\sum_{j=1}^n(\varsigma\overline{w}+\overline{\varepsilon}_{f,j})^2$, $\overline{w}=\sqrt{\sum_{j=1}^n\overline{w}_j^2}$, $\underline{\sigma}=\inf_i\underline{\sigma}_i$ and $d_0=\ln(1/\varsigma),0<\varsigma\leq 1$.

Proof: Note that the high-order term $\mathbf{h}(\mathbf{z};\widetilde{\mathbf{c}},\widetilde{\boldsymbol{\sigma}})$ in (34) can be derived from

$$\begin{aligned}\mathbf{h}(\mathbf{z};\widetilde{\mathbf{c}},\widetilde{\boldsymbol{\sigma}}) &= \boldsymbol{\Phi}_1^*-\widehat{\boldsymbol{\Phi}}-\boldsymbol{\Phi}_{\mathbf{c}}'(\mathbf{c}_1^*-\widehat{\mathbf{c}})-\boldsymbol{\Phi}_{\boldsymbol{\sigma}}'(\boldsymbol{\sigma}_1^*-\widehat{\boldsymbol{\sigma}})\\ &= \widetilde{\boldsymbol{\Phi}}-\boldsymbol{\Phi}_{\mathbf{c}}'\widetilde{\mathbf{c}}-\boldsymbol{\Phi}_{\boldsymbol{\sigma}}'\widetilde{\boldsymbol{\sigma}}.\end{aligned} \tag{36}$$

Substituting (36) into (34), we have

$$\begin{aligned}\boldsymbol{\varepsilon}_f^T\boldsymbol{\varepsilon}_f &= \left(\widehat{\mathbf{W}}^T\left(\widetilde{\boldsymbol{\Phi}}-\boldsymbol{\Phi}_{\mathbf{c}}'\widetilde{\mathbf{c}}-\boldsymbol{\Phi}_{\boldsymbol{\sigma}}'\widetilde{\boldsymbol{\sigma}}\right)+\widetilde{\mathbf{W}}^T\widetilde{\boldsymbol{\Phi}}+\widehat{\boldsymbol{\varepsilon}}_f^*\right)^T\\ &\quad\times\left(\widehat{\mathbf{W}}^T\left(\widetilde{\boldsymbol{\Phi}}-\boldsymbol{\Phi}_{\mathbf{c}}'\widetilde{\mathbf{c}}-\boldsymbol{\Phi}_{\boldsymbol{\sigma}}'\widetilde{\boldsymbol{\sigma}}\right)+\widetilde{\mathbf{W}}^T\widetilde{\boldsymbol{\Phi}}+\widehat{\boldsymbol{\varepsilon}}_f^*\right)\\ &= \left(\widetilde{\boldsymbol{\Phi}}-\boldsymbol{\Phi}_{\mathbf{c}}'\widetilde{\mathbf{c}}-\boldsymbol{\Phi}_{\boldsymbol{\sigma}}'\widetilde{\boldsymbol{\sigma}}\right)^T\widehat{\mathbf{W}}\widehat{\mathbf{W}}^T\left(\widetilde{\boldsymbol{\Phi}}-\boldsymbol{\Phi}_{\mathbf{c}}'\widetilde{\mathbf{c}}-\boldsymbol{\Phi}_{\boldsymbol{\sigma}}'\widetilde{\boldsymbol{\sigma}}\right)\\ &\quad+\widetilde{\boldsymbol{\Phi}}^T\widetilde{\mathbf{W}}\widetilde{\mathbf{W}}^T\widetilde{\boldsymbol{\Phi}}+(\widehat{\boldsymbol{\varepsilon}}_f^*)^T\widehat{\boldsymbol{\varepsilon}}_f^*\\ &\quad+2\left(\widetilde{\boldsymbol{\Phi}}-\boldsymbol{\Phi}_{\mathbf{c}}'\widetilde{\mathbf{c}}-\boldsymbol{\Phi}_{\boldsymbol{\sigma}}'\widetilde{\boldsymbol{\sigma}}\right)^T\widehat{\mathbf{W}}\widetilde{\mathbf{W}}^T\widetilde{\boldsymbol{\Phi}}\\ &\quad+2\left(\widetilde{\boldsymbol{\Phi}}-\boldsymbol{\Phi}_{\mathbf{c}}'\widetilde{\mathbf{c}}-\boldsymbol{\Phi}_{\boldsymbol{\sigma}}'\widetilde{\boldsymbol{\sigma}}\right)^T\widehat{\mathbf{W}}\widehat{\boldsymbol{\varepsilon}}_f^*+2\widetilde{\boldsymbol{\Phi}}^T\widetilde{\mathbf{W}}\widehat{\boldsymbol{\varepsilon}}_f^*\\ &= \widetilde{\boldsymbol{\Phi}}^T\widehat{\mathbf{W}}\widehat{\mathbf{W}}^T\widetilde{\boldsymbol{\Phi}}+\widetilde{\mathbf{c}}^T(\boldsymbol{\Phi}_{\mathbf{c}}')^T\widehat{\mathbf{W}}\widehat{\mathbf{W}}^T\boldsymbol{\Phi}_{\mathbf{c}}'\widetilde{\mathbf{c}}\\ &\quad+\widetilde{\boldsymbol{\sigma}}^T(\boldsymbol{\Phi}_{\boldsymbol{\sigma}}')^T\widehat{\mathbf{W}}\widehat{\mathbf{W}}^T\boldsymbol{\Phi}_{\boldsymbol{\sigma}}'\widetilde{\boldsymbol{\sigma}}+\widetilde{\boldsymbol{\Phi}}^T\widetilde{\mathbf{W}}\widetilde{\mathbf{W}}^T\widetilde{\boldsymbol{\Phi}}+(\widehat{\boldsymbol{\varepsilon}}_f^*)^T\widehat{\boldsymbol{\varepsilon}}_f^*\\ &\quad+2\widetilde{\boldsymbol{\Phi}}^T\widehat{\mathbf{W}}\widetilde{\mathbf{W}}^T\widetilde{\boldsymbol{\Phi}}+2\widetilde{\mathbf{c}}^T(\boldsymbol{\Phi}_{\mathbf{c}}')^T\widehat{\mathbf{W}}\widehat{\mathbf{W}}^T\boldsymbol{\Phi}_{\boldsymbol{\sigma}}'\widetilde{\boldsymbol{\sigma}}\\ &\quad-2\widetilde{\mathbf{c}}^T(\boldsymbol{\Phi}_{\mathbf{c}}')^T\widehat{\mathbf{W}}(\mathbf{W}_1^*)^T\widetilde{\boldsymbol{\Phi}}-2\widetilde{\boldsymbol{\sigma}}^T(\boldsymbol{\Phi}_{\boldsymbol{\sigma}}')^T\widehat{\mathbf{W}}(\mathbf{W}_1^*)^T\widetilde{\boldsymbol{\Phi}}\\ &\quad+2\widetilde{\boldsymbol{\Phi}}^T\mathbf{W}_1^*\widehat{\boldsymbol{\varepsilon}}_f^*-2\widetilde{\mathbf{c}}^T(\boldsymbol{\Phi}_{\mathbf{c}}')^T\widehat{\mathbf{W}}\widehat{\boldsymbol{\varepsilon}}_f^*-2\widetilde{\boldsymbol{\sigma}}^T(\boldsymbol{\Phi}_{\boldsymbol{\sigma}}')^T\widehat{\mathbf{W}}\widehat{\boldsymbol{\varepsilon}}_f^*.\end{aligned} \tag{37}$$

Using the following inequalities:

$$2\widetilde{\boldsymbol{\Phi}}^T\widehat{\mathbf{W}}\widetilde{\mathbf{W}}^T\widetilde{\boldsymbol{\Phi}} \le \widetilde{\boldsymbol{\Phi}}^T\widehat{\mathbf{W}}\widehat{\mathbf{W}}^T\widetilde{\boldsymbol{\Phi}} + \widetilde{\boldsymbol{\Phi}}^T\widetilde{\mathbf{W}}\widetilde{\mathbf{W}}^T\widetilde{\boldsymbol{\Phi}} \quad (38)$$

$$2\widetilde{\mathbf{c}}^T(\boldsymbol{\Phi}'_{\mathbf{c}})^T\widehat{\mathbf{W}}\widehat{\mathbf{W}}^T\boldsymbol{\Phi}'_{\boldsymbol{\sigma}}\widetilde{\boldsymbol{\sigma}} \le \widetilde{\mathbf{c}}^T(\boldsymbol{\Phi}'_{\mathbf{c}})^T\widehat{\mathbf{W}}\widehat{\mathbf{W}}^T\boldsymbol{\Phi}'_{\mathbf{c}}\widetilde{\mathbf{c}} + \widetilde{\boldsymbol{\sigma}}^T(\boldsymbol{\Phi}'_{\boldsymbol{\sigma}})^T\widehat{\mathbf{W}}\widehat{\mathbf{W}}^T\boldsymbol{\Phi}'_{\boldsymbol{\sigma}}\widetilde{\boldsymbol{\sigma}} \quad (39)$$

$$-2\widetilde{\mathbf{c}}^T(\boldsymbol{\Phi}'_{\mathbf{c}})^T\widehat{\mathbf{W}}(\mathbf{W}_1^*)^T\widetilde{\boldsymbol{\Phi}} \le \widetilde{\mathbf{c}}^T(\boldsymbol{\Phi}'_{\mathbf{c}})^T\widehat{\mathbf{W}}\widehat{\mathbf{W}}^T\boldsymbol{\Phi}'_{\mathbf{c}}\widetilde{\mathbf{c}} + \widetilde{\boldsymbol{\Phi}}^T\mathbf{W}_1^*(\mathbf{W}_1^*)^T\widetilde{\boldsymbol{\Phi}} \quad (40)$$

$$-2\widetilde{\boldsymbol{\sigma}}^T(\boldsymbol{\Phi}'_{\boldsymbol{\sigma}})^T\widehat{\mathbf{W}}(\mathbf{W}_1^*)^T\widetilde{\boldsymbol{\Phi}} \le \widetilde{\boldsymbol{\sigma}}^T(\boldsymbol{\Phi}'_{\boldsymbol{\sigma}})^T\widehat{\mathbf{W}}\widehat{\mathbf{W}}^T\boldsymbol{\Phi}'_{\boldsymbol{\sigma}}\widetilde{\boldsymbol{\sigma}} + \widetilde{\boldsymbol{\Phi}}^T\mathbf{W}_1^*(\mathbf{W}_1^*)^T\widetilde{\boldsymbol{\Phi}} \quad (41)$$

$$2\widetilde{\boldsymbol{\Phi}}^T\mathbf{W}_1^*\widehat{\boldsymbol{\varepsilon}}_f^* \le (\widehat{\boldsymbol{\varepsilon}}_f^*)^T\widehat{\boldsymbol{\varepsilon}}_f^* + \widetilde{\boldsymbol{\Phi}}^T\mathbf{W}_1^*(\mathbf{W}_1^*)^T\widetilde{\boldsymbol{\Phi}} \quad (42)$$

$$-2\widetilde{\mathbf{c}}^T(\boldsymbol{\Phi}'_{\mathbf{c}})^T\widehat{\mathbf{W}}\widehat{\boldsymbol{\varepsilon}}_f^* \le \widetilde{\mathbf{c}}^T(\boldsymbol{\Phi}'_{\mathbf{c}})^T\widehat{\mathbf{W}}\widehat{\mathbf{W}}^T\boldsymbol{\Phi}'_{\mathbf{c}}\widetilde{\mathbf{c}} + (\widehat{\boldsymbol{\varepsilon}}_f^*)^T\widehat{\boldsymbol{\varepsilon}}_f^* \quad (43)$$

$$-2\widetilde{\boldsymbol{\sigma}}^T(\boldsymbol{\Phi}'_{\boldsymbol{\sigma}})^T\widehat{\mathbf{W}}\widehat{\boldsymbol{\varepsilon}}_f^* \le \widetilde{\boldsymbol{\sigma}}^T(\boldsymbol{\Phi}'_{\boldsymbol{\sigma}})^T\widehat{\mathbf{W}}\widehat{\mathbf{W}}^T\boldsymbol{\Phi}'_{\boldsymbol{\sigma}}\widetilde{\boldsymbol{\sigma}} + (\widehat{\boldsymbol{\varepsilon}}_f^*)^T\widehat{\boldsymbol{\varepsilon}}_f^*. \quad (44)$$

We rewrite (37) as follows:

$$\begin{aligned}\boldsymbol{\varepsilon}_f^T\boldsymbol{\varepsilon}_f \le\ & 4\widetilde{\mathbf{c}}^T(\boldsymbol{\Phi}'_{\mathbf{c}})^T\widehat{\mathbf{W}}\widehat{\mathbf{W}}^T\boldsymbol{\Phi}'_{\mathbf{c}}\widetilde{\mathbf{c}} + 4\widetilde{\boldsymbol{\sigma}}^T(\boldsymbol{\Phi}'_{\boldsymbol{\sigma}})^T\widehat{\mathbf{W}}\widehat{\mathbf{W}}^T\boldsymbol{\Phi}'_{\boldsymbol{\sigma}}\widetilde{\boldsymbol{\sigma}} \\ & + 2\widetilde{\boldsymbol{\Phi}}^T\widetilde{\mathbf{W}}\widetilde{\mathbf{W}}^T\widetilde{\boldsymbol{\Phi}} + 2\widetilde{\boldsymbol{\Phi}}^T\widehat{\mathbf{W}}\widehat{\mathbf{W}}^T\widetilde{\boldsymbol{\Phi}} \\ & + 3\widetilde{\boldsymbol{\Phi}}^T\mathbf{W}_1^*(\mathbf{W}_1^*)^T\widetilde{\boldsymbol{\Phi}} + 4(\widehat{\boldsymbol{\varepsilon}}_f^*)^T\widehat{\boldsymbol{\varepsilon}}_f^*. \end{aligned} \quad (45)$$

Note that

$$\begin{aligned}&\lambda_{\max}\left((\boldsymbol{\Phi}'_{\mathbf{c}})^T\widehat{\mathbf{W}}\widehat{\mathbf{W}}^T\boldsymbol{\Phi}'_{\mathbf{c}}\right) \\ &\quad \le \overline{w}^2\lambda_{\max}\left(\operatorname{diag}\left(\boldsymbol{\phi}_{\mathbf{c}_1}\boldsymbol{\phi}_{\mathbf{c}_1}^T,\ldots,\boldsymbol{\phi}_{\mathbf{c}_N}\boldsymbol{\phi}_{\mathbf{c}_N}^T\right)\right) \le \frac{2d_0\overline{w}^2}{\underline{\sigma}^2} \end{aligned} \quad (46)$$

$$\begin{aligned}&\lambda_{\max}\left((\boldsymbol{\Phi}'_{\boldsymbol{\sigma}})^T\widehat{\mathbf{W}}\widehat{\mathbf{W}}^T\boldsymbol{\Phi}'_{\boldsymbol{\sigma}}\right) \\ &\quad \le \overline{w}^2\lambda_{\max}\left(\operatorname{diag}\left(\boldsymbol{\phi}_{\boldsymbol{\sigma}_1}\boldsymbol{\phi}_{\boldsymbol{\sigma}_1}^T,\ldots,\boldsymbol{\phi}_{\boldsymbol{\sigma}_N}\boldsymbol{\phi}_{\boldsymbol{\sigma}_N}^T\right)\right) \le \frac{2d_0^2\overline{w}^2}{\underline{\sigma}^2}. \end{aligned} \quad (47)$$

Together with (45), it is not difficult to see that (35) holds. This concludes the proof. □

Remark 3: In comparison with previous approximation analysis of [47] and [53]–[57], whereby reconstruction errors are either directly assumed to be bounded or implicitly shown with conservative bounds, Theorem 1 explicitly presents the upper bound (35) of SCFNN-based approximation with respect to parameter estimate errors, and thereby facilitating stability analysis of the overall SARFNC system.

C. Adaptive Laws

To avoid parameter drift and guarantee parameter boundedness that $\|\boldsymbol{\omega}_j\| \le \overline{\omega}_j$, $j = 1, 2, \ldots, n$, $\underline{c}_i \le c_i^l \le \overline{c}_i$ and $0 < \underline{\sigma}_i \le \sigma_i^l \le \overline{\sigma}_i, i = 1, 2, \ldots, m, l = 1, 2, \ldots, N$, the adaptive laws using the projection modification for parameters $\widehat{\boldsymbol{\omega}}_j$, $\widehat{c}_i^l$, and $\widehat{\sigma}_i^l$ are designed as follows:

$$\dot{\widehat{\boldsymbol{\omega}}}_j = \begin{cases} \eta_w s_j\widehat{\boldsymbol{\Phi}}, & \text{if } \|\widehat{\boldsymbol{\omega}}_j\| < \overline{\omega}_j \\ & \text{or } \left(\|\widehat{\boldsymbol{\omega}}_j\| = \overline{\omega}_j \text{ and } s_j\widehat{\boldsymbol{\omega}}_j^T\widehat{\boldsymbol{\Phi}} \le 0\right) \\ \eta_w s_j\widehat{\boldsymbol{\Phi}} - \eta_w s_j\widehat{\boldsymbol{\omega}}_j^T\widehat{\boldsymbol{\Phi}}\widehat{\boldsymbol{\omega}}_j/\|\widehat{\boldsymbol{\omega}}_j\|^2, & \text{otherwise} \end{cases} \quad (48)$$

$$\dot{\widehat{c}}_i^l = \begin{cases} \eta_c\phi_i^{c,l}\widehat{\mathbf{w}}_l^T\mathbf{s}, & \text{if } \underline{c}_i < \widehat{c}_i^l < \overline{c}_i \\ & \text{or } \left(\widehat{c}_i^l = \underline{c}_i \text{ and } \phi_i^{c,l}\widehat{\mathbf{w}}_l^T\mathbf{s} \ge 0\right) \\ & \text{or } \left(\widehat{c}_i^l = \overline{c}_i \text{ and } \phi_i^{c,l}\widehat{\mathbf{w}}_l^T\mathbf{s} \le 0\right) \\ 0, & \text{otherwise} \end{cases} \quad (49)$$

$$\dot{\widehat{\sigma}}_i^l = \begin{cases} \eta_\sigma\phi_i^{\sigma,l}\widehat{\mathbf{w}}_l^T\mathbf{s}, & \text{if } \underline{\sigma}_i < \widehat{\sigma}_i^l < \overline{\sigma}_i \\ & \text{or } \left(\widehat{\sigma}_i^l = \underline{\sigma}_i \text{ and } \phi_i^{\sigma,l}\widehat{\mathbf{w}}_l^T\mathbf{s} \ge 0\right) \\ & \text{or } \left(\widehat{\sigma}_i^l = \overline{\sigma}_i \text{ and } \phi_i^{\sigma,l}\widehat{\mathbf{w}}_l^T\mathbf{s} \le 0\right) \\ 0, & \text{otherwise} \end{cases} \quad (50)$$

where $\widehat{\boldsymbol{\omega}}_j = [\widehat{\omega}_j^1, \ldots, \widehat{\omega}_j^N]^T$ and $\widehat{\mathbf{w}}_l = [\widehat{w}_1^l, \ldots, \widehat{w}_n^l]^T$.

Remark 4: Due to the dynamic partitioning of the SCFNN, the fuzzy sets or hidden neurons with fixed parameters can hardly guarantee optimal accommodation of online observations, and thereby leading to poor identification. In this context, it is highly desired that all the parameters of the SCFNN approximator are updated simultaneously for accurate approximation.

Remark 5: Unlike traditional adaptive laws modified by the bounded norm, the improved projection-based adaptive laws in (48)–(50) are designed to ensure that the centers are updated within the universe of discourse and the widths are positively bounded in each dimension, respectively. In addition to center parameter drift, the singularity in membership functions can be avoided effectively.

Remark 6: Although system states $\mathbf{z} = [\boldsymbol{\eta}^T, \dot{\boldsymbol{\eta}}^T]^T$ of the closed-loop SARFNC system are eventually bounded on $U_{\mathbf{z}}$, it does not imply that parameter estimates $\widehat{\boldsymbol{\omega}}_j$, $\widehat{c}_i^l$, and $\widehat{\sigma}_i^l$ are finitely bounded since the width $\widehat{\sigma}_i^l$ and the center $\widehat{c}_i^l$ might approach to zero and infinity, respectively, if the aforementioned projection modifications in (48)–(50) are removed.

D. Stability Analysis

It is essential that when the SARFNC scheme is applied to track the surface vehicle, the closed-loop system is stable. The key result ensuring closed-loop stability is stated here.

Theorem 2: Consider the surface vehicle dynamics (5) with the proposed SARFNC control scheme using (23)–(25), and the adaptive laws for parameter updates using (48)–(50), where online approximation $\widehat{\mathbf{f}}_{\mathrm{F}}$ is realized by the SCFNN scheme (26). Then, the tracking error $\mathbf{e}(t)$ and its derivative $\dot{\mathbf{e}}(t)$ are GUUB and can be made arbitrarily small. Moreover, all parameters $\widehat{\mathbf{W}}$, $\widehat{\mathbf{c}}$, and $\widehat{\boldsymbol{\sigma}}$ and actual tracking states $\boldsymbol{\eta}$ and $\dot{\boldsymbol{\eta}}$ are bounded.

Proof: Substituting (23) and (24) into (5) yields

$$\dot{\mathbf{s}} = \widetilde{\mathbf{W}}^T\widehat{\boldsymbol{\Phi}} + \widehat{\mathbf{W}}^T\boldsymbol{\Phi}'_{\mathbf{c}}\widetilde{\mathbf{c}} + \widehat{\mathbf{W}}^T\boldsymbol{\Phi}'_{\boldsymbol{\sigma}}\widetilde{\boldsymbol{\sigma}} + \boldsymbol{\varepsilon}_f + \mathbf{G}\boldsymbol{\tau}_{\mathrm{rsc}}. \quad (51)$$

Consider the following Lyapunov function:

$$V_2 = \frac{1}{2}\left[\mathbf{s}^T\mathbf{s} + \frac{\operatorname{tr}(\widetilde{\mathbf{W}}^T\widetilde{\mathbf{W}})}{\eta_w} + \frac{\widetilde{\mathbf{c}}^T\widetilde{\mathbf{c}}}{\eta_c} + \frac{\widetilde{\boldsymbol{\sigma}}^T\widetilde{\boldsymbol{\sigma}}}{\eta_\sigma}\right]. \quad (52)$$

Differentiating V_2 with respect to time t and using (51), we have

$$\begin{aligned}\dot{V}_2 =\ & \mathbf{s}^T\left(\widetilde{\mathbf{W}}^T\widehat{\boldsymbol{\Phi}} + \widehat{\mathbf{W}}^T\boldsymbol{\Phi}'_{\mathbf{c}}\widetilde{\mathbf{c}} + \widehat{\mathbf{W}}^T\boldsymbol{\Phi}'_{\boldsymbol{\sigma}}\widetilde{\boldsymbol{\sigma}} + \boldsymbol{\varepsilon}_f + \mathbf{G}\boldsymbol{\tau}_{\mathrm{rsc}}\right) \\ & - \eta_w^{-1}\operatorname{tr}(\widetilde{\mathbf{W}}^T\dot{\widehat{\mathbf{W}}}) - \eta_c^{-1}\widetilde{\mathbf{c}}^T\dot{\widehat{\mathbf{c}}} - \eta_\sigma^{-1}\widetilde{\boldsymbol{\sigma}}^T\dot{\widehat{\boldsymbol{\sigma}}} \\ =\ & \left(\sum_{j=1}^n s_j\widetilde{\boldsymbol{\omega}}_j^T\right)\widehat{\boldsymbol{\Phi}} - \eta_w^{-1}\sum_{j=1}^n\widetilde{\boldsymbol{\omega}}_j^T\dot{\widehat{\boldsymbol{\omega}}}_j + \widetilde{\mathbf{c}}^T(\boldsymbol{\Phi}'_{\mathbf{c}})^T\widehat{\mathbf{W}}\mathbf{s} \\ & - \eta_c^{-1}\widetilde{\mathbf{c}}^T\dot{\widehat{\mathbf{c}}} + \widetilde{\boldsymbol{\sigma}}^T(\boldsymbol{\Phi}'_{\boldsymbol{\sigma}})^T\widehat{\mathbf{W}}\mathbf{s} - \eta_\sigma^{-1}\widetilde{\boldsymbol{\sigma}}^T\dot{\widehat{\boldsymbol{\sigma}}} \\ & + \mathbf{s}^T(\boldsymbol{\varepsilon}_f + \mathbf{G}\boldsymbol{\tau}_{\mathrm{rsc}}) \end{aligned}$$

$$= \sum_{j=1}^{n} \widetilde{\boldsymbol{\omega}}_j^T \left(s_j \widehat{\boldsymbol{\Phi}} - \eta_w^{-1} \dot{\widehat{\boldsymbol{\omega}}}_j\right) + \widetilde{\mathbf{c}}^T \left((\boldsymbol{\Phi}_{\mathbf{c}}')^T \widehat{\mathbf{W}} \mathbf{s} - \eta_c^{-1} \dot{\widehat{\mathbf{c}}}\right) + \widetilde{\boldsymbol{\sigma}}^T \left((\boldsymbol{\Phi}_{\boldsymbol{\sigma}}')^T \widehat{\mathbf{W}} \mathbf{s} - \eta_\sigma^{-1} \dot{\widehat{\boldsymbol{\sigma}}}\right) + \mathbf{s}^T (\boldsymbol{\varepsilon}_f + \mathbf{G}\boldsymbol{\tau}_{\text{rsc}}).$$

Furthermore, we have

$$\dot{V}_2 = \underbrace{\sum_{j=1}^{n} \widetilde{\boldsymbol{\omega}}_j^T \left(s_j \widehat{\boldsymbol{\Phi}} - \eta_w^{-1} \dot{\widehat{\boldsymbol{\omega}}}_j\right)}_{\text{term}_1} + \underbrace{\sum_{i,l=1,1}^{m,N} \widetilde{c}_i^l \left(\phi_i^{c,l} \widehat{\mathbf{w}}_l^T \mathbf{s} - \eta_c^{-1} \dot{\widehat{c}}_i^l\right)}_{\text{term}_2} + \underbrace{\sum_{i,l=1,1}^{m,N} \widetilde{\sigma}_i^l \left(\phi_i^{\sigma,l} \widehat{\mathbf{w}}_l^T \mathbf{s} - \eta_\sigma^{-1} \dot{\widehat{\sigma}}_i^l\right)}_{\text{term}_3} + \mathbf{s}^T \left(\boldsymbol{\varepsilon}_f - \frac{\delta^2+1}{2\delta^2} \boldsymbol{\Gamma} \mathbf{s}\right). \tag{53}$$

1) Term 1: Consider the case $\|\widehat{\boldsymbol{\omega}}_{j_1}\| < \overline{\omega}_{j_1}$ or $(\|\widehat{\boldsymbol{\omega}}_{j_1}\| = \overline{\omega}_{j_1}$ and $s_{j_1} \widehat{\boldsymbol{\omega}}_{j_1}^T \widehat{\boldsymbol{\Phi}} \le 0)$, where $\mathcal{J}_1 = \{j_1\} \subseteq \mathcal{J} = \{1, 2, \ldots, n\}$. By (48), we have

$$\sum_{j \in \mathcal{J}_1} \widetilde{\boldsymbol{\omega}}_j^T \left(s_j \widehat{\boldsymbol{\Phi}} - \eta_w^{-1} \dot{\widehat{\boldsymbol{\omega}}}_j\right) = 0. \tag{54}$$

Otherwise, i.e., if $\|\widehat{\boldsymbol{\omega}}_{j_2}\| \ge \overline{\omega}_{j_2} \ge \|\boldsymbol{\omega}_{j_2}^*\|$ and $s_{j_2} \widehat{\boldsymbol{\omega}}_{j_2}^T \widehat{\boldsymbol{\Phi}} > 0$, where $\mathcal{J}_2 = \{j_2\} \subseteq \mathcal{J}$. By (48), we have

$$\begin{aligned} &\sum_{j \in \mathcal{J}_2} \widetilde{\boldsymbol{\omega}}_j^T \left(s_j \widehat{\boldsymbol{\Phi}} - \eta_w^{-1} \dot{\widehat{\boldsymbol{\omega}}}_j\right) \\ &= \sum_{j \in \mathcal{J}_2} \widetilde{\boldsymbol{\omega}}_j^T \left(s_j \widehat{\boldsymbol{\omega}}_j^T \widehat{\boldsymbol{\Phi}} \widehat{\boldsymbol{\omega}}_j / \|\widehat{\boldsymbol{\omega}}_j\|\right) \\ &= \sum_{j \in \mathcal{J}_2} s_j \widehat{\boldsymbol{\omega}}_j^T \widehat{\boldsymbol{\Phi}} \left(\boldsymbol{\omega}_j^* - \widehat{\boldsymbol{\omega}}_j\right)^T \widehat{\boldsymbol{\omega}}_j / \|\widehat{\boldsymbol{\omega}}_j\| \\ &= -\frac{1}{2} \sum_{j \in \mathcal{J}_2} s_j \widehat{\boldsymbol{\omega}}_j^T \widehat{\boldsymbol{\Phi}} \left(\|\widehat{\boldsymbol{\omega}}_j\|^2 - \|\boldsymbol{\omega}_j^*\|^2 + \|\widehat{\boldsymbol{\omega}}_j - \boldsymbol{\omega}_j^*\|^2\right) / \|\widehat{\boldsymbol{\omega}}_j\| \\ &\le 0. \end{aligned} \tag{55}$$

Combining (54) with (55), we obtain

$$\begin{aligned} \text{term}_1 &= \sum_{j \in \mathcal{J}_1} \widetilde{\boldsymbol{\omega}}_j^T \left(s_j \widehat{\boldsymbol{\Phi}} - \eta_w^{-1} \dot{\widehat{\boldsymbol{\omega}}}_j\right) + \sum_{j \in \mathcal{J}_2} \widetilde{\boldsymbol{\omega}}_j^T \left(s_j \widehat{\boldsymbol{\Phi}} - \eta_w^{-1} \dot{\widehat{\boldsymbol{\omega}}}_j\right) \\ &\le 0. \end{aligned} \tag{56}$$

2) Term 2: From (49), if there exist $(i_1, l_1) \in \mathcal{I}_1^c \subseteq \{1, 2, \ldots, m\} \times \{1, 2, \ldots, N\}$ such that $0 < \underline{c}_{i_1} < \widehat{c}_{i_1}^{l_1} < \overline{c}_{i_1}$ or $(\widehat{c}_{i_1}^{l_1} = \underline{c}_{i_1}$ and $\phi_{i_1}^{c,l_1} \widehat{\mathbf{w}}_{l_1}^T \mathbf{s} \ge 0)$ or $(\widehat{c}_{i_1}^{l_1} = \overline{c}_{i_1}$ and $\phi_{i_1}^{c,l_1} \widehat{\mathbf{w}}_{l_1}^T \mathbf{s} \le 0)$, we have

$$\sum_{(i,l) \in \mathcal{I}_1^c} \widetilde{c}_i^l \left(\phi_i^{c,l} \widehat{\mathbf{w}}_l^T \mathbf{s} - \eta_c^{-1} \dot{\widehat{c}}_i^l\right) = 0. \tag{57}$$

Otherwise, if there exist $(i_2, l_2) \in \mathcal{I}_2^c \subseteq \{1, 2, \ldots, m\} \times \{1, 2, \ldots, N\}$ such that $(\widehat{c}_{i_2}^{l_2} \le \underline{c}_{i_2} \le c_{i_2}^{l_2 *}$ and $\phi_{i_2}^{c,l_2} \widehat{\mathbf{w}}_{l_2}^T \mathbf{s} < 0)$ or $(c_{i_2}^{l_2 *} \ge \widehat{c}_{i_2}^{l_2} \ge \overline{c}_{i_2}$ and $\phi_{i_2}^{c,l_2} \widehat{\mathbf{w}}_{l_2}^T \mathbf{s} > 0)$, we have

$$\sum_{(i,l) \in \mathcal{I}_2^c} \widetilde{c}_i^l \left(\phi_i^{c,l} \widehat{\mathbf{w}}_l^T \mathbf{s} - \eta_c^{-1} \dot{\widehat{c}}_i^l\right) = \sum_{(i,l) \in \mathcal{I}_2^c} \widetilde{c}_i^l \phi_i^{c,l} \widehat{\mathbf{w}}_l^T \mathbf{s} \le 0. \tag{58}$$

Combining (57) with (58), we have

$$\begin{aligned} \text{term}_2 &= \sum_{(i,l) \in \mathcal{I}_1^c} \widetilde{c}_i^l \left(\phi_i^{c,l} \widehat{\mathbf{w}}_l^T \mathbf{s} - \eta_c^{-1} \dot{\widehat{c}}_i^l\right) + \sum_{(i,l) \in \mathcal{I}_2^c} \widetilde{c}_i^l \left(\phi_i^{c,l} \widehat{\mathbf{w}}_l^T \mathbf{s} - \eta_c^{-1} \dot{\widehat{c}}_i^l\right) \\ &\le 0. \end{aligned} \tag{59}$$

3) Term 3: From (50), if there exist $(i_1, l_1) \in \mathcal{I}_1^\sigma \subseteq \{1, 2, \ldots, m\} \times \{1, 2, \ldots, N\}$ such that $0 < \underline{\sigma}_{i_1} < \widehat{\sigma}_{i_1}^{l_1} < \overline{\sigma}_{i_1}$ or $(\widehat{\sigma}_{i_1}^{l_1} = \underline{\sigma}_{i_1}$ and $\phi_{i_1}^{\sigma,l_1} \widehat{\mathbf{w}}_{l_1}^T \mathbf{s} \ge 0)$ or $(\widehat{\sigma}_{i_1}^{l_1} = \overline{\sigma}_{i_1}$ and $\phi_{i_1}^{\sigma,l_1} \widehat{\mathbf{w}}_{l_1}^T \mathbf{s} \le 0)$, we have

$$\sum_{(i,l) \in \mathcal{I}_1^\sigma} \widetilde{\sigma}_i^l \left(\phi_i^{\sigma,l} \widehat{\mathbf{w}}_l^T \mathbf{s} - \eta_\sigma^{-1} \dot{\widehat{\sigma}}_i^l\right) = 0. \tag{60}$$

Otherwise, if there exist $(i_2, l_2) \in \mathcal{I}_2^\sigma \subseteq \{1, 2, \ldots, m\} \times \{1, 2, \ldots, N\}$ such that $(\widehat{\sigma}_{i_2}^{l_2} \le \underline{\sigma}_{i_2} \le \sigma_{i_2}^{l_2 *}$ and $\phi_{i_2}^{\sigma,l_2} \widehat{\mathbf{w}}_{l_2}^T \mathbf{s} < 0)$ or $(\sigma_{i_2}^{l_2 *} \ge \widehat{\sigma}_{i_2}^{l_2} \ge \overline{\sigma}_{i_2}$ and $\phi_{i_2}^{\sigma,l_2} \widehat{\mathbf{w}}_{l_2}^T \mathbf{s} > 0)$, we have

$$\sum_{(i,l) \in \mathcal{I}_2^\sigma} \widetilde{\sigma}_i^l \left(\phi_i^{\sigma,l} \widehat{\mathbf{w}}_l^T \mathbf{s} - \eta_\sigma^{-1} \dot{\widehat{\sigma}}_i^l\right) = \sum_{(i,l) \in \mathcal{I}_2^\sigma} \widetilde{\sigma}_i^l \phi_i^{\sigma,l} \widehat{\mathbf{w}}_l^T \mathbf{s} \le 0. \tag{61}$$

Combining (60) with (61), we have

$$\begin{aligned} \text{term}_3 &= \sum_{(i,l) \in \mathcal{I}_1^\sigma} \widetilde{\sigma}_i^l \left(\phi_i^{\sigma,l} \widehat{\mathbf{w}}_l^T \mathbf{s} - \eta_\sigma^{-1} \dot{\widehat{\sigma}}_i^l\right) + \sum_{(i,l) \in \mathcal{I}_2^\sigma} \widetilde{\sigma}_i^l \left(\phi_i^{\sigma,l} \widehat{\mathbf{w}}_l^T \mathbf{s} - \eta_\sigma^{-1} \dot{\widehat{\sigma}}_i^l\right) \\ &\le 0. \end{aligned} \tag{62}$$

Choose the Lyapunov function of the sliding surface as follows:

$$V_1 = \frac{1}{2} \mathbf{s}^T \mathbf{s}. \tag{63}$$

Applying (56), (59), (62), and (63) to (53), we have

$$\begin{aligned} \dot{V}_2 \le \dot{V}_1 &= \mathbf{s}^T \dot{\mathbf{s}} \\ &= \mathbf{s}^T \left(\boldsymbol{\varepsilon}_f - \frac{\delta^2+1}{2\delta^2} \boldsymbol{\Gamma} \mathbf{s}\right) \\ &= \mathbf{s}^T \boldsymbol{\varepsilon}_f - \frac{\delta^2+1}{2\delta^2} \mathbf{s}^T \boldsymbol{\Gamma} \mathbf{s} \\ &= -\frac{1}{2} \mathbf{s}^T \boldsymbol{\Gamma} \mathbf{s} - \frac{1}{2} \left(\frac{\mathbf{s}}{\delta} - \delta \boldsymbol{\Gamma}^{-1} \boldsymbol{\varepsilon}_f\right)^T \boldsymbol{\Gamma} \left(\frac{\mathbf{s}}{\delta} - \delta \boldsymbol{\Gamma}^{-1} \boldsymbol{\varepsilon}_f\right) \\ &\quad + \frac{1}{2} \delta^2 \boldsymbol{\varepsilon}_f^T \boldsymbol{\Gamma}^{-1} \boldsymbol{\varepsilon}_f \\ &\le -\frac{1}{2} \mathbf{s}^T \boldsymbol{\Gamma} \mathbf{s} + \frac{1}{2} \delta^2 \boldsymbol{\varepsilon}_f^T \boldsymbol{\Gamma}^{-1} \boldsymbol{\varepsilon}_f. \end{aligned} \tag{64}$$

Substituting (35) into (64), we have

$$\begin{aligned}\dot{V}_1 &\le -\frac{1}{2}\mathbf{s}^T\boldsymbol{\Gamma}\mathbf{s}+\frac{1}{2}\delta^2\boldsymbol{\varepsilon}_f^T\boldsymbol{\Gamma}^{-1}\boldsymbol{\varepsilon}_f \\ &\le \lambda_{\min}^{-1}(\boldsymbol{\Gamma})\left(-\frac{\lambda_{\min}^2(\boldsymbol{\Gamma})}{2}\mathbf{s}^T\mathbf{s}+\frac{1}{2}\delta^2\boldsymbol{\varepsilon}_f^T\boldsymbol{\varepsilon}_f\right) \\ &\le \lambda_{\min}(\boldsymbol{\Gamma})\left[\begin{array}{l}-\frac{1}{2}\mathbf{s}^T\mathbf{s}+\frac{\delta^2}{2\lambda_{\min}^2(\boldsymbol{\Gamma})} \\ \times\left(\begin{array}{c}\frac{8d_0\overline{w}^2}{\underline{\sigma}^2}\widetilde{\mathbf{c}}^T\widetilde{\mathbf{c}}+\frac{8d_0^2\overline{w}^2}{\underline{\sigma}^2}\widetilde{\boldsymbol{\sigma}}^T\widetilde{\boldsymbol{\sigma}} \\ +2\mathrm{tr}(\widetilde{\mathbf{W}}^T\widetilde{\mathbf{W}})+\Delta d\end{array}\right)\end{array}\right] \\ &= -\alpha V_1+\rho(\widetilde{\mathbf{W}},\widetilde{\mathbf{c}},\widetilde{\boldsymbol{\sigma}}). \end{aligned} \tag{65}$$

Note that $\widetilde{\mathbf{W}}$, $\widetilde{\mathbf{c}}$, and $\widetilde{\boldsymbol{\sigma}}$ are bounded if corresponding initial conditions $\mathbf{s}(0)$, $\widehat{\mathbf{W}}(0)$, $\widehat{\mathbf{c}}(0)$, and $\widehat{\boldsymbol{\sigma}}(0)$ are bounded. From the boundedness of $\mathbf{W}^*$, $\mathbf{c}^*$, and $\boldsymbol{\sigma}^*$, we have that parameter estimates $\widehat{\mathbf{W}}$, $\widehat{\mathbf{c}}$, and $\widehat{\boldsymbol{\sigma}}$ are bounded. By (64) and (65), we have

$$0 \le V_1(t) \le \frac{\rho}{\alpha}+\left(V_1(0)-\frac{\rho}{\alpha}\right)e^{-\alpha t}. \tag{66}$$

It implies that $V_1(t)$ is GUUB, and thereby rendering the error surface $\mathbf{s}$ being GUUB

$$\|\mathbf{s}\| \le \sqrt{\frac{2\rho}{\alpha}+2\left(V_1(0)-\frac{\rho}{\alpha}\right)e^{-\alpha t}}. \tag{67}$$

Moreover, there exists a time constant $T_{\mathbf{s}} > 0$, for any $\mu_{\mathbf{s}} > \sqrt{2\rho/\alpha}$, such that $\|\mathbf{s}\| \le \mu_{\mathbf{s}}$, where the bound $\mu_{\mathbf{s}}$ can be made arbitrarily small since ρ/α can be rendered arbitrarily small if parameters η_w, η_c, η_σ, δ, $\boldsymbol{\Gamma}$, and $\mathbf{K}$ are selected appropriately. According to (22), it follows that the tracking error $\mathbf{e}(t)$ and its derivative $\dot{\mathbf{e}}(t)$ can achieve arbitrary accuracy. From the boundedness of reference signals $\boldsymbol{\eta}_d$ and $\dot{\boldsymbol{\eta}}_d$, we have that actual tracking states $\boldsymbol{\eta}$ and $\dot{\boldsymbol{\eta}}$ are bounded.

It follows that the proposed SARFNC scheme (23) using (24) and (25) together with (48)–(50) guarantee not only accurate trajectory tracking but also parameter convergence and boundedness. This concludes the proof. □

Remark 7: Note that the upper bound is governed by $\rho/\alpha = \delta^2/\lambda_{\min}^2(\|\widetilde{\mathbf{W}}\|_F^2+\beta_c\|\widetilde{\mathbf{c}}\|^2+\beta_\sigma\|\widetilde{\boldsymbol{\sigma}}\|^2+\Delta d/2)$, where $\beta_c = 4d_0\overline{w}^2/\underline{\sigma}^2$ and $\beta_\sigma = 4d_0^2\overline{w}^2/\underline{\sigma}^2$. Accordingly, large γ_i and small δ would render the upper bound of tracking errors small. Moreover, update gains η_w, η_c, and η_σ are employed to drive parallel parameter estimates $\widehat{\mathbf{W}}$, $\widehat{\mathbf{c}}$, and $\widehat{\boldsymbol{\sigma}}$ to their optimal values, and thereby contributing to high accuracies in both approximation and tracking. Actually, parameters η_w, η_c, and η_σ are only associated with the rates of the adaptation with projection modification in (48)–(50) which avoid parameter drift and ensure stable learning process. In this context, larger η_w, η_c, and η_σ result in more rapid responses, and do not destroy the closed-loop stability. Usually, the gains η_w, η_c, and η_σ do not need fine tuning and can be freely chosen from a wide range.

V. Simulation Studies

To demonstrate the effectiveness and superiority of the SARFNC scheme, we conduct simulation studies on the well-known ship model CyberShip II [5], which is a 1:70 scale replica of a supply ship of the Marine Cybernetics Laboratory at the Norwegian University of Science and Technology. Its main parameters are listed in Table I.

TABLE I
Main Parameters of the CyberShip II

m	23.8000	Y_v	−0.8612	$X_{\dot{u}}$	−2.0
I_z	1.7600	$Y_{\|v\|v}$	−36.2823	$Y_{\dot{v}}$	−10.0
x_g	0.0460	Y_r	0.1079	$Y_{\dot{r}}$	−0.0
X_u	−0.7225	N_v	0.1052	$N_{\dot{v}}$	−0.0
$X_{\|u\|u}$	−1.3274	$N_{\|v\|v}$	5.0437	$N_{\dot{r}}$	−1.0
X_{uuu}	−5.8664				

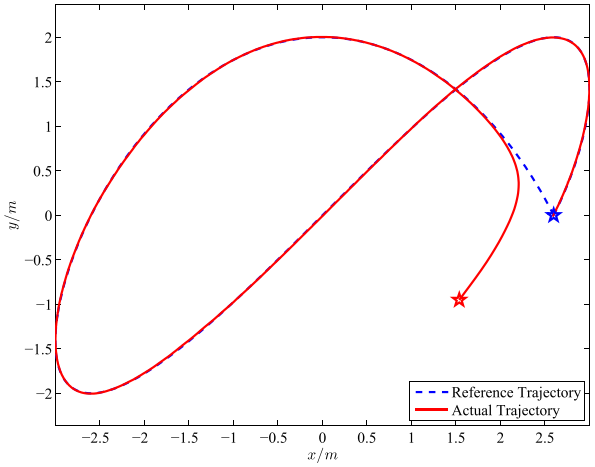

Fig. 4. Reference and actual trajectories in the xy plane.

In this section, our objective is to track exactly the smooth trajectory $\boldsymbol{\eta}_d(t)$ and its derivative $\dot{\boldsymbol{\eta}}_d(t)$ given by

$$\boldsymbol{\eta}_d(t) = \begin{bmatrix} 3\cos(0.02\pi t+\pi/6) \\ 2\sin(0.03\pi t) \\ \pi+\pi\sin(0.04\pi t-\pi/6)\end{bmatrix}. \tag{68}$$

The unknown external environmental disturbances $\mathbf{b}(t)$ with large magnitude and high frequency are governed by

$$\mathbf{b}(t) = \begin{bmatrix} 5\sin(0.1\pi t-\pi/4) \\ 8\cos(0.1\pi t+\pi/6) \\ 2\sin(0.1\pi t+\pi/3)\end{bmatrix} \tag{69}$$

and the initial conditions of the vessel are set as follows:

$$\begin{aligned}\mathbf{z}(0) &= [\boldsymbol{\eta}^T(0),\dot{\boldsymbol{\eta}}^T(0)]^T \\ &= [1.5(\mathrm{m}),-1(\mathrm{m}),0(\mathrm{rad}),0(\mathrm{m/s}),0(\mathrm{m/s}),0(\mathrm{rad/s})]^T.\end{aligned}$$

The design parameters of the SARFNC are chosen as follows: $\mathbf{K}_1 = \mathbf{K}_2 = \mathrm{diag}(0.8,0.8,0.4)$, $\epsilon = 0.9$, $\varsigma = 0.1$, $\overline{\omega}_j = 2$, $\eta_w = 10$, $\eta_c = 5$, $\eta_\sigma = 5$, $\overline{c}_i = 6$, $\underline{c}_i = -3$, $\overline{\sigma}_i = 5$, $\underline{\sigma}_i = 0.1$, $\delta = 0.5$, $\boldsymbol{\Gamma} = \mathrm{diag}(1,1,1)$, $\boldsymbol{\sigma}_{\mathrm{init}} = [2,1.5,3,0.2,0.1,0.5]^T$, and $\mathbf{w}_{\mathrm{init}} = \mathbf{0}$.

The actual and reference trajectories in the planar space are shown in Fig. 4, from which we can observe that the proposed SARFNC control system can track the desired trajectory with high accuracy. The states $\boldsymbol{\eta} = [x,y,\psi]^T$ and $\dot{\boldsymbol{\eta}} = [\dot{x},\dot{y},\dot{\psi}]^T$ together with their desired targets are shown in Figs. 5 and 6, respectively, from which we can observe that the actual states are able to track the desired ones with rapid transient response and high steady-state accuracy. The corresponding

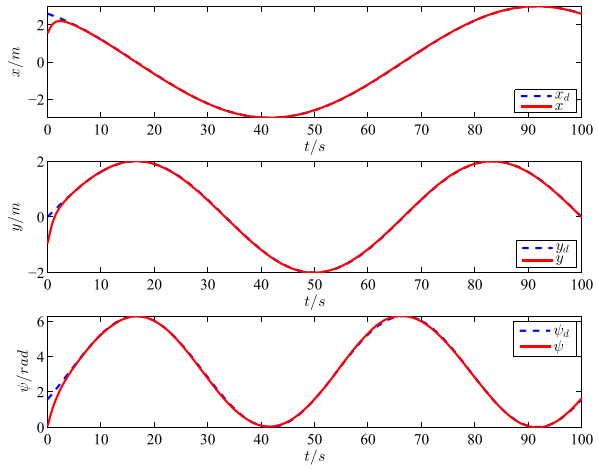

Fig. 5. Desired and actual states x, y, and ψ.

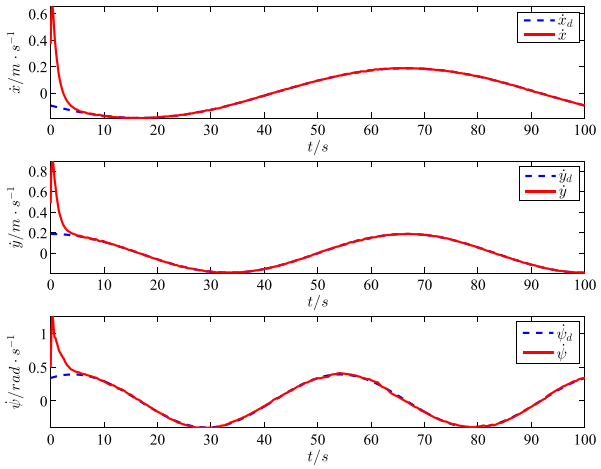

Fig. 6. Desired and actual states $\dot{x}$, $\dot{y}$, and $\dot{\psi}$.

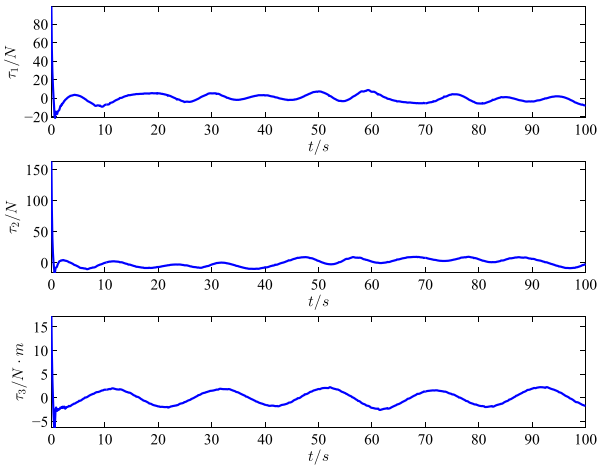

Fig. 7. Control forces τ_1, τ_2, and torque τ_3.

control forces and torque $\boldsymbol{\tau} = [\tau_1, \tau_2, \tau_3]^T$ from the SARFNC scheme are shown in Fig. 7, which demonstrates that the smooth control actions dynamically vary with the unknown nonlinear dynamics f_1, f_2, and f_3, which are in turn strongly disturbed by the external signal $\mathbf{b}(t)$. The remarkable control performance of the SARFNC scheme actually results from

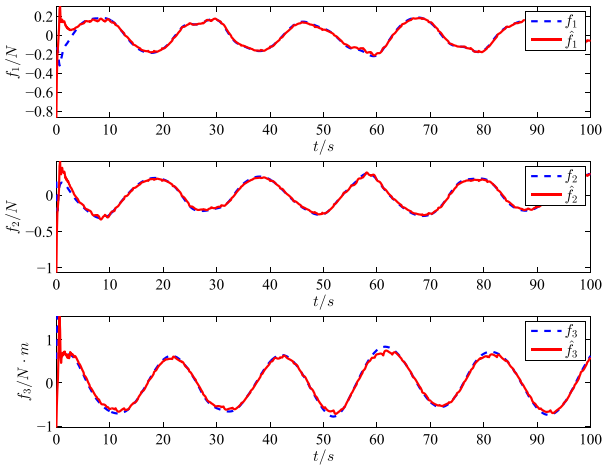

Fig. 8. Dynamics f_1, f_2, and f_3 and SCFNN-based approximation $\widehat{f}_1$, $\widehat{f}_2$, and $\widehat{f}_3$.

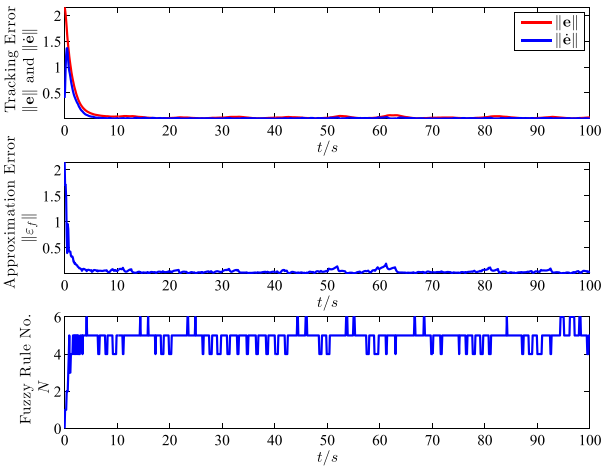

Fig. 9. Online tracking, approximation errors, and fuzzy rule numbers.

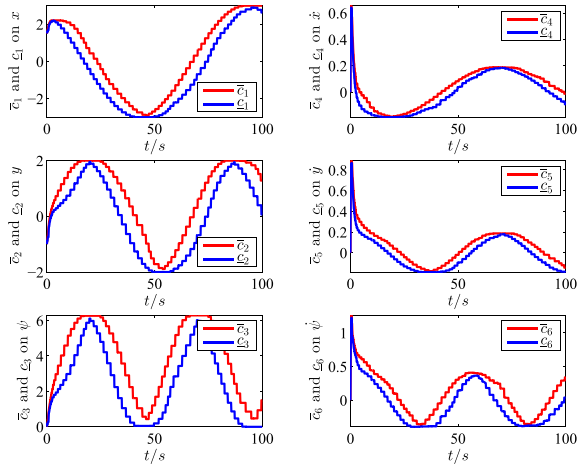

Fig. 10. Center bounds $\overline{c}_i, \underline{c}_i$, $i = 1, 2, \ldots, 6$.

the online approximation ability of the SCFNN scheme which is shown in Fig. 8. Moreover, the online tracking errors $\|\mathbf{e}\|$, $\|\dot{\mathbf{e}}\|$, approximation error $\|\boldsymbol{\varepsilon}_f\|$, and fuzzy rule number $N(t)$ are shown Fig. 9, which demonstrates that the dynamic SCFNN-based SARFNC with compact fuzzy rules guarantees

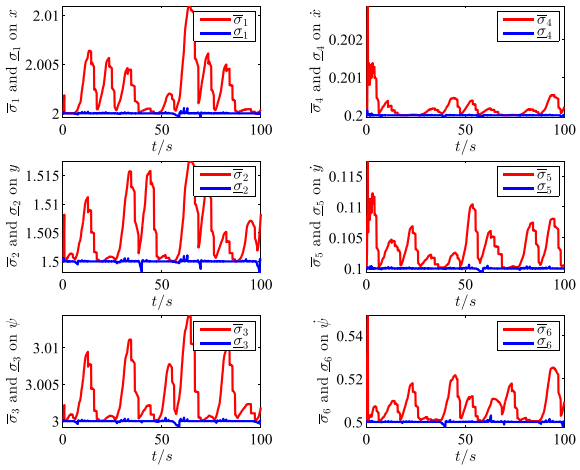

Fig. 11. Width bounds $\overline{\sigma}_i, \underline{\sigma}_i, i = 1, 2, \ldots, 6$.

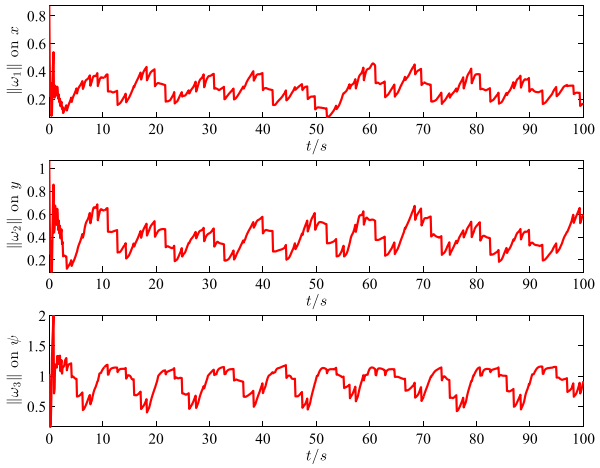

Fig. 12. Output weight norms $\|\boldsymbol{\omega}_j\|, j = 1, 2, 3$.

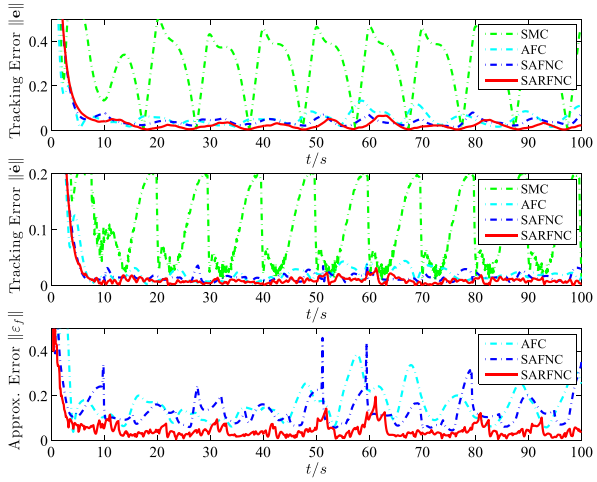

Fig. 13. Comparisons on tracking and approximation errors.

convergent tracking errors and bounded approximation error simultaneously. In addition, the parameter boundedness of $\overline{c}_i, \underline{c}_i, \overline{\sigma}_i, \underline{\sigma}_i, \|\boldsymbol{\omega}_j\|$ as shown in Figs. 10–12, is guaranteed.

To demonstrate the superiority of the SARFNC scheme, we make comprehensive comparisons with the existing

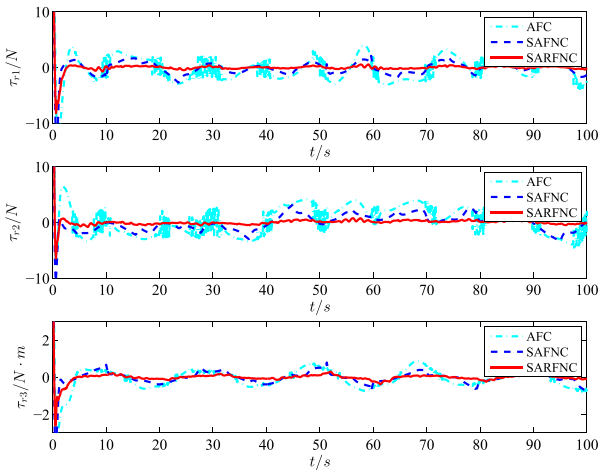

Fig. 14. Comparisons on robust compensation forces and torque.

TABLE II
PERFORMANCE COMPARISONS OF SARFNC WITH SMC, AFC, AND SAFNC

Performance		SARFNC	SMC [4]	AFC [19]	SAFNC [53]
IAE	e_1	**1.5792**	3.5434	2.2860	2.7447
	e_2	**1.5415**	3.0645	2.6963	3.0307
	e_3	**4.9695**	30.6460	6.2789	5.0394
	$\dot{e}_1$	**1.2130**	3.3291	1.4480	1.5082
	$\dot{e}_2$	**1.1532**	2.9098	1.6340	1.4405
	$\dot{e}_3$	**2.3140**	11.4220	3.4591	2.6832
ITAE	e_1	**12.8963**	33.5719	228.5988	58.5426
	e_2	**17.9783**	34.8660	269.6339	79.2924
	e_3	**110.7301**	1483.1022	627.8905	147.0014
	$\dot{e}_1$	**6.7107**	88.5929	144.7995	23.5746
	$\dot{e}_2$	**8.2836**	85.8542	163.4047	25.4582
	$\dot{e}_3$	**44.3588**	482.2620	345.9094	63.3892
IAE	$\varepsilon_{f,1}$	**1.6151**	–	4.0225	4.1237
	$\varepsilon_{f,2}$	**1.7293**	–	5.7788	5.5316
	$\varepsilon_{f,3}$	**4.6368**	–	15.1656	10.3318
ITAE	$\varepsilon_{f,1}$	**41.9484**	–	402.2451	180.0138
	$\varepsilon_{f,2}$	**60.3927**	–	577.8844	257.3420
	$\varepsilon_{f,3}$	**184.4977**	–	1516.5577	476.6681

control methods including the SMC of [4], adaptive fuzzy control (AFC) of [19] with fixed structure and self-organizing adaptive fuzzy neural control (SAFNC) [53] with dynamic structure. Note that the AFC adopts 64 fuzzy rules using two fuzzy sets in each input and allows centers, widths, and output weights to be updated online by adaptive laws, while the SAFNC scheme finally involves 15 fuzzy rules. The tracking errors $\|\mathbf{e}\|, \|\dot{\mathbf{e}}\|$ and approximation error $\|\boldsymbol{\varepsilon}_f\|$ are shown in Fig. 13, from which we can observe that the SARFNC preserves minimal errors of tracking control and dynamics identification with very short settling time. Moreover, it should be highlighted that the SCFNN-based rule construction mechanism and the projection-based adaptive laws of the SARFNC guarantee that the meaningful widths are positive and bounded in the universe of discourse in addition that the centers and output weights are bounded.

It should be noted that the AAC dominates the SARFNC while the RSC forces (shown in Fig. 14) significantly compensate the initial approximation errors and nearly vanish when accurate approximation is achieved. As shown in Fig. 14, in comparison with robust compensation in the AFC and SAFNC,

the RSC forces and torques demonstrate that the SARFNC requires minor compensation (i.e., more robust) since the SCFNN-based approximation can achieve high accuracy after short initial learning. However, the AFC and SAFNC need to perform dominant compensation for suppressing large approximation errors at all times, and may even suffer from severe chattering.

Performance comparisons on the aforementioned simulation results are summarized in Table II, where the integrated absolute error (IAE) and integrated time absolute error (ITAE) defined as IAE $= \int_0^t |e(\tau)|d\tau$ and ITAE $= \int_0^t t|e(\tau)|d\tau$, respectively, are used to evaluate the transient and steady-state performances in online tracking and approximation. It is evident that the SARFNC scheme using online self-organizing fuzzy rules performs much better than the SAFNC scheme with dynamic fuzzy rules, the AFC with limited approximation by a predefined structure, and the SMC scheme without identification for unknown dynamics. In terms of tracking accuracy, the performance of SARFNC scheme is remarkably superior to that of the SAFNC, AFC, and SMC in both transient and steady-state responses since the corresponding IAE and ITAE indices of the SARFNC are significantly smaller than those of others. It follows that the proposed SARFNC is able to track the reference trajectory with an excellent accuracy by virtue of accurate approximation to system uncertainties and unknown disturbances.

VI. Conclusion

In this paper, a novel SARFNC scheme for trajectory tracking of surface vehicles in the presence of system uncertainties and unknown time-varying disturbances has been proposed. The SARFNC scheme is comprised of an AAC and an RSC, whereby the AAC is realized by combining a sliding-mode surface of tracking errors with an online approximator based on a SCFNN while the RSC is used to suppress corresponding approximation errors. To be more specific, the SCFNN is implemented by employing dynamically constructive fuzzy rules according to the structure learning criteria including generation and pruning of rules. Using adaptive projection-based update laws for all free parameters of the SCFNN, i.e., centers, widths, and output weights, all the widths of the fuzzy sets in individual input variables are rendered to be strictly positive and bounded in addition that all centers and output weights are updated within the universe of discourse. Moreover, it has been proven that the tracking error $\mathbf{e}(t)$ and its derivative $\dot{\mathbf{e}}(t)$ of the SARFNC control system are GUUB. Simulation studies and comprehensive comparisons with SMC, AFC with fixed structure, and SAFNC with dynamic structure are conducted on the CyberShip II model. Simulation results demonstrate that the SARFNC achieves remarkably superior performances in both trajectory tracking and uncertainty approximation in terms of transient and steady-state responses, simultaneously.

Acknowledgment

The authors would like to thank the Editor-in-Chief, Associate Editor, and the anonymous referees for their invaluable comments and suggestions.

References

[1] T. I. Fossen, *Marine Control Systems: Guidance, Navigation, and Control of Ships, Rigs and Underwater Vehicles*. Trondheim, Norway: Marine Cybernetics AS, 2002.

[2] H. K. Khalil, *Nonlinear Systems*, 2nd ed. Upper Saddle River, NJ, USA: Prentice-Hall, 1996.

[3] M. Kristic, I. Kanellakopoulos, and P. V. Kokotović, *Nonlinear and Adaptive Control Design*. New York, NY, USA: Wiley, 1995.

[4] J.-J. Slotine and W. Li, *Applied Nonlinear Control*. Englewood Cliffs, NJ, USA: Prentice-Hall, 1991.

[5] R. Skjetne, T. I. Fossen, and P. V. Kokotović, "Adaptive maneuvering, with experiments, for a model ship in a marine control laboratory," *Automatica*, vol. 41, no. 2, pp. 289–298, Feb. 2005.

[6] N. Wang, M. Han, N. Dong, and M. J. Er, "Constructive multi-output extreme learning machine with application to large tanker motion dynamics identification," *Neurocomputing*, vol. 128, pp. 59–72, Mar. 2014.

[7] T. Holzhüter, "LQG approach for the high-precision track control of ships," *IEE Proc.-Control Theory Appl.*, vol. 144, no. 2, pp. 121–127, Mar. 1997.

[8] B. Vik and T. I. Fossen, "Semiglobal exponential output feedback control of ships," *IEEE Trans. Control Syst. Technol.*, vol. 5, no. 3, pp. 360–370, May 1997.

[9] M. Wondergem, E. Lefeber, K. Y. Pettersen, and H. Nijmeijer, "Output feedback tracking of ships," *IEEE Trans. Control Syst. Technol.*, vol. 19, no. 2, pp. 442–448, Mar. 2011.

[10] R. Zhang, Y. Chen, Z. Sun, F. Sun, and H. Xu, "Path control of a surface ship in restricted waters using sliding mode," *IEEE Trans. Control Syst. Technol.*, vol. 8, no. 4, pp. 722–732, Jul. 2000.

[11] Z.-P. Jiang, "Global tracking control of underactuated ships by Lyapunov's direct method," *Automatica*, vol. 38, no. 2, pp. 301–309, Feb. 2002.

[12] H. Ashrafiuon, K. R. Muske, L. C. McNinch, and R. A. Soltan, "Sliding-mode tracking control of surface vessels," *IEEE Trans. Ind. Electron.*, vol. 55, no. 11, pp. 4004–4012, Nov. 2008.

[13] L. C. McNinch, H. Ashrafiuon, and K. R. Muske, "Optimal specification of sliding mode control parameters for unmanned surface vessel systems," in *Proc. Amer. Control Conf.*, Villanova, PA, USA, 2009, pp. 2350–2355.

[14] E. Lefeber, K. Y. Pettersen, and H. Nijmeijer, "Tracking control of an underactuated ship," *IEEE Trans. Control Syst. Technol.*, vol. 11, no. 1, pp. 52–61, Jan. 2003.

[15] Z. Li, J. Sun, and S. Oh, "Design, analysis and experimental validation of a robust nonlinear path following controller for marine surface vessels," *Automatica*, vol. 45, no. 7, pp. 1649–1658, Jul. 2009.

[16] W. Wang, J. Yi, D. Zhao, and D. Liu, "Design of a stable sliding-mode controller for a class of second-order underactuated systems," *IEE Proc.-Control Theory Appl.*, vol. 151, no. 6, pp. 683–690, Nov. 2004.

[17] R. Yu, Q. Zhu, G. Xia, and Z. Liu, "Sliding mode tracking control of an underactuated surface vessel," *IET Control Theory Appl.*, vol. 6, no. 3, pp. 461–466, Feb. 2012.

[18] K. D. Do and J. Pan, *Control of Ships and Underwater Vehicles: Design for Underactuated and Nonlinear Marine Systems*. London, U.K.: Springer-Verlag, 2009.

[19] S. Tong and H. X. Li, "Fuzzy adaptive sliding-mode control for MIMO nonlinear systems," *IEEE Trans. Fuzzy Syst.*, vol. 11, no. 3, pp. 354–360, Jun. 2003.

[20] T.-S. Li, S.-C. Tong, and G. G. Feng, "A novel robust adaptive-fuzzy-tracking control for a class of nonlinearmulti-input/multi-output systems," *IEEE Trans. Fuzzy Syst.*, vol. 18, no. 1, pp. 150–160, Feb. 2010.

[21] Y.-J. Liu, W. Wang, S.-C. Tong, and Y.-S. Liu, "Robust adaptive tracking control for nonlinear systems based on bounds of fuzzy approximation parameters," *IEEE Trans. Syst., Man, Cybern. A, Syst., Humans*, vol. 40, no. 1, pp. 170–184, Jan. 2010.

[22] S.-C. Tong, Y.-M. Li, G. Feng, and T.-S. Li, "Observer-based adaptive fuzzy backstepping dynamic surface control for a class of MIMO nonlinear systems," *IEEE Trans. Syst., Man, Cybern. B, Cybern.*, vol. 41, no. 4, pp. 1124–1135, Aug. 2011.

[23] S. S. Ge and C. Wang, "Direct adaptive NN control of a class of nonlinear systems," *IEEE Trans. Neural Netw.*, vol. 13, no. 1, pp. 214–221, Jan. 2002.

[24] M. Chen, S. S. Ge, and B. Voon Ee How, "Robust adaptive neural network control for a class of uncertain MIMO nonlinear systems with input nonlinearities," *IEEE Trans. Neural Netw.*, vol. 21, no. 5, pp. 796–812, May 2010.

[25] Y.-J. Liu, S.-C. Tong, D. Wang, T.-S. Li, and C. L. P. Chen, "Adaptive neural output feedback controller design with reduced-order observer for a class of uncertain nonlinear SISO systems," *IEEE Trans. Neural Netw.*, vol. 22, no. 8, pp. 1328–1334, Aug. 2011.

[26] J. Na, X. Ren, and D. Zheng, "Adaptive control for nonlinear pure-feedback systems with high-order sliding mode observer," *IEEE Trans. Neural Netw. Learn. Syst.*, vol. 24, no. 3, pp. 370–382, Mar. 2013.

[27] B. Xu, C. G. Yang, and Z. K. Shi, "Reinforcement learning output feedback NN control using deterministic learning technique," *IEEE Trans. Neural Netw. Learn. Syst.*, vol. 25, no. 3, pp. 635–641, Mar. 2014.

[28] C. G. Yang, S. S. Ge, C. Xiang, T. Chai, and T. Lee, "Output feedback NN control for two classes of discrete-time systems with unknown control directions in a unified approach," *IEEE Trans. Neural Netw.*, vol. 19, no. 11, pp. 1873–1886, Nov. 2008.

[29] W. Y. Wang, M. L. Chan, C. C. J. Hsu, and T. T. Lee, "H_∞ tracking-based sliding mode control for uncertain nonlinear systems via an adaptive fuzzy-neural approach," *IEEE Trans. Syst. Man Cybern. B, Cybern.*, vol. 32, no. 4, pp. 483–492, Aug. 2002.

[30] R.-J. Lian, "Adaptive self-organizing fuzzy sliding-mode radial basis-function neural-network controller for robotic systems," *IEEE Trans. Ind. Electron.*, vol. 61, no. 3, pp. 1493–1503, Mar. 2014.

[31] Z. Liu and C. Li, "Fuzzy neural network quadratic stabilization output feedback control for biped robots via H_∞ approach," *IEEE Trans. Syst. Man Cybern. B, Cybern.*, vol. 33, no. 1, pp. 67–84, Feb. 2003.

[32] F. Sun, L. Li, H.-X. Li, and H. Liu, "Neuro-fuzzy dynamic-inversion-based adaptive control for robotic manipulators—Discrete time case," *IEEE Trans. Ind. Electron.*, vol. 54, no. 3, pp. 1342–1351, Jun. 2007.

[33] S.-J. Huang and W.-C. Lin, "Adaptive fuzzy controller with sliding surface for vehicle suspension control," *IEEE Trans. Fuzzy Syst.*, vol. 11, no. 4, pp. 550–559, Aug. 2003.

[34] E. Kim, "Output feedback tracking control of robot manipulators with model uncertainty via adaptive fuzzy logic," *IEEE Trans. Fuzzy Syst.*, vol. 12, no. 3, pp. 368–378, Jun. 2004.

[35] L.-X. Wang, "Stable adaptive fuzzy controllers with application to inverted pendulum tracking," *IEEE Trans. Syst., Man, Cybern. B, Cybern.*, vol. 26, no. 5, pp. 677–691, Oct. 1996.

[36] J. Fei and J. Zhou, "Robust adaptive control of MEMS triaxial gyroscope using fuzzy compensator," *IEEE Trans. Syst., Man, Cybern. B, Cybern.*, vol. 42, no. 6, pp. 1599–1607, Dec. 2012.

[37] J. R. Layne and K. M. Passino, "Fuzzy model reference learning control for cargo ship steering," *IEEE Control Syst.*, vol. 13, no. 6, pp. 23–34, Dec. 1993.

[38] J. Velagic, Z. Vukic, and E. Omerdic, "Adaptive fuzzy ship autopilot for track-keeping," *J. Control Eng. Pract.*, vol. 11, no. 4, pp. 433–443, Apr. 2003.

[39] R. S. Burns, "The use of artificial neural networks for the intelligent optimal control of surface ships," *IEEE J. Oceanic Eng.*, vol. 20, no. 1, pp. 65–72, Jan. 1995.

[40] A. Leonessa, T. VanZwieten, and Y. Morel, "Neural network model reference adaptive control of marine vehicles," in *Current Trends in Nonlinear Systems and Control*. Boston, MA, USA: Birkhäuser, 2006, pp. 421–440.

[41] Y. Yang and J. Ren, "Adaptive fuzzy robust tracking controller design via small gain approach and its application," *IEEE Trans. Fuzzy Syst.*, vol. 11, no. 6, pp. 783–795, Dec. 2003.

[42] K. P. Tee and S. S. Ge, "Control of fully actuated ocean surface vessels using a class of feedforward approximators," *IEEE Trans. Control Syst. Technol.*, vol. 14, no. 4, pp. 750–756, Jul. 2006.

[43] S.-L. Dai, C. Wang, and F. Luo, "Identification and learning control of ocean surface ship using neural networks," *IEEE Trans. Ind. Inform.*, vol. 8, no. 4, pp. 801–810, Nov. 2012.

[44] W.-Y. Wang, Y.-H. Chien, Y.-G. Leu, and T.-T. Lee, "Adaptive T-S fuzzy-neural modeling and control for general MIMO unknown nonaffine nonlinear systems using projection update laws," *Automatica*, vol. 46, no. 5, pp. 852–863, May 2010.

[45] Y. Pan, M. J. Er, D. Huang, and Q. Wang, "Adaptive fuzzy control with guaranteed convergence of optimal approximation error," *IEEE Trans. Fuzzy Syst.*, vol. 19, no. 5, pp. 807–818, Oct. 2011.

[46] J. A. Farrell and M. M. Polycarpou, *Adaptive Approximation Based Control: Unifying Neural, Fuzzy and Traditional Adaptive Approximation Approaches*. Hoboken, NJ, USA: Wiley, 2006.

[47] J.-H. Park, S.-H. Huh, S.-H. Kim, S.-J. Seo, and G.-T. Park, "Direct adaptive controller for nonaffine nonlinear systems using self-structuring neural networks," *IEEE Trans. Neural Netw.*, vol. 16, no. 2, pp. 414–422, Mar. 2005.

[48] J.-H. Park, G.-T. Park, S.-H. Kim, and C.-J. Moon, "Output-feedback control of uncertain nonlinear systems using a self-structuring adaptive fuzzy observer," *Fuzzy Sets Syst.*, vol. 151, no. 1, pp. 21–42, Apr. 2005.

[49] N. Wang, M. J. Er, and X. Meng, "A fast and accurate online self-organizing scheme for parsimonious fuzzy neural networks," *Neurocomputing*, vol. 72, nos. 16–18, pp. 3818–3829, Dec. 2009.

[50] N. Wang, M. J. Er, X.-Y. Meng, and X. Li, "An online self-organizing scheme for parsimonious and accurate fuzzy neural networks," *Int. J. Neural Syst.*, vol. 20, no. 5, pp. 389–405, Oct. 2010.

[51] N. Wang, "A generalized ellipsoidal basis function based online self-constructing fuzzy neural network," *Neural Process. Lett.*, vol. 34, no. 1, pp. 13–37, Aug. 2011.

[52] Y. Gao and M. J. Er, "Online adaptive fuzzy neural identification and control of a class of MIMO nonlinear systems," *IEEE Trans. Fuzzy Syst.*, vol. 11, no. 4, pp. 462–477, Aug. 2003.

[53] C.-F. Hsu, "Self-organizing adaptive fuzzy neural control for a class of nonlinear systems," *IEEE Trans. Neural Netw.*, vol. 18, no. 4, pp. 1232–1241, Jul. 2007.

[54] C.-S. Chen, "Dynamic structure neural-fuzzy networks for robust adaptive control of robot manipulators," *IEEE Trans. Ind. Electron.*, vol. 55, no. 9, pp. 3402–3414, Sep. 2008.

[55] C.-S. Chen, "Robust self-organizing neural-fuzzy control with uncertainty observer for MIMO nonlinear systems," *IEEE Trans. Fuzzy Syst.*, vol. 19, no. 4, pp. 694–706, Aug. 2011.

[56] C.-H. Wang and K.-N. Hung, "Intelligent adaptive law for missile guidance using fuzzy neural networks," *Int. J. Fuzzy Syst.*, vol. 15, no. 2, pp. 182–191, Jun. 2013.

[57] Y.-C. Wang, C.-J. Chien, and C.-C. Teng, "Direct adaptive iterative learning control of nonlinear systems using an output-recurrent fuzzy neural network," *IEEE Trans. Syst., Man, Cybern. B, Cybern.*, vol. 34, no. 3, pp. 1348–1359, Jun. 2004.

Ning Wang (S'08–M'12) received the B.Eng. degree in marine engineering and the Ph.D. degree in control theory and engineering from Dalian Maritime University (DMU), Dalian, China, in 2004 and 2009, respectively.

He was financially supported by the China Scholarship Council to work as a joint training Ph.D. student with Nanyang Technological University (NTU), Singapore, from 2008 to 2009. He is currently an Associate Professor with the Marine Engineering College, DMU. His current research interests include fuzzy logic systems, artificial neural networks, machine learning, self-organizing fuzzy neural modeling and control, ship intelligent control, and dynamic ship navigational safety assessment.

Dr. Wang was a recipient of the Nomination Award of Liaoning Province Excellent Doctoral Dissertation, the DMU Excellent Doctoral Dissertation Award, and the DMU Outstanding Ph.D. Student Award in 2010. He was also a recipient of the Liaoning Province Award for Technological Invention, and the Honor of Liaoning BaiQianWan Talents, Liaoning Excellent Talents, and Dalian Leading Talents. In light of his significant research at NTU, he received the Excellent Government-Funded Scholars and Students Award in 2009. He currently serves as an Associate Editor of the *Neurocomputing*.

Meng Joo Er (S'82–M'87–SM'07) is currently a Full Professor of Electrical and Electronic Engineering with Nanyang Technological University, Singapore. He has authored five books, 16 book chapters, and over 500 refereed journal and conference papers. His current research interests include computational intelligence, robotics and automation, sensor networks, biomedical engineering, and cognitive science.

Dr. Er received the Institution of Engineers Singapore (IES) Prestigious Engineering Achievement Award 2011, in recognition of the significant and impactful contributions to Singapore's development by his research project entitled *Development of Intelligent Techniques for Modeling, Controlling and Optimizing Complex Manufacturing Systems*. He is also the only dual winner in Singapore IES Prestigious Publication Award in Application in 1996 and the IES Prestigious Publication Award in Theory in 2001. He currently serves as the Editor-in-Chief of the *Transactions on Machine Learning and Artificial Intelligence*, an Associate Editor of 11 refereed international journals, including the IEEE TRANSACTIONS ON FUZZY SYSTEMS and the IEEE TRANSACTIONS ON CYBERNETICS.